

**Evolutionary ecology and discovery of new bioactive compounds from
Lumnitzera mangroves across the Indonesian Archipelago**

Der Fakultät für Lebenswissenschaften

der Universität Leipzig

eingereichte

DISSERTATION

zur Erlangung des akademischen Grades

Doctor rerum naturalium

(Dr. rer. nat.)

Vorgelegt von

M.Sc. Jeprianto Manurung

geboren am 24.07.1989 in Cahaya Pardomuan, Indonesia

Dekan: Prof. Dr. Marc Schönwiesner

Gutachter: Prof. Dr. Alexandra Muellner-Riehl

Prof. Dr. Nicole van Dam

Tag der Verteidigung: 28.10.2022

Supporting information

All supplementary material I this document are available online in <https://www.mdpi.com/2297-8739/8/6/82>

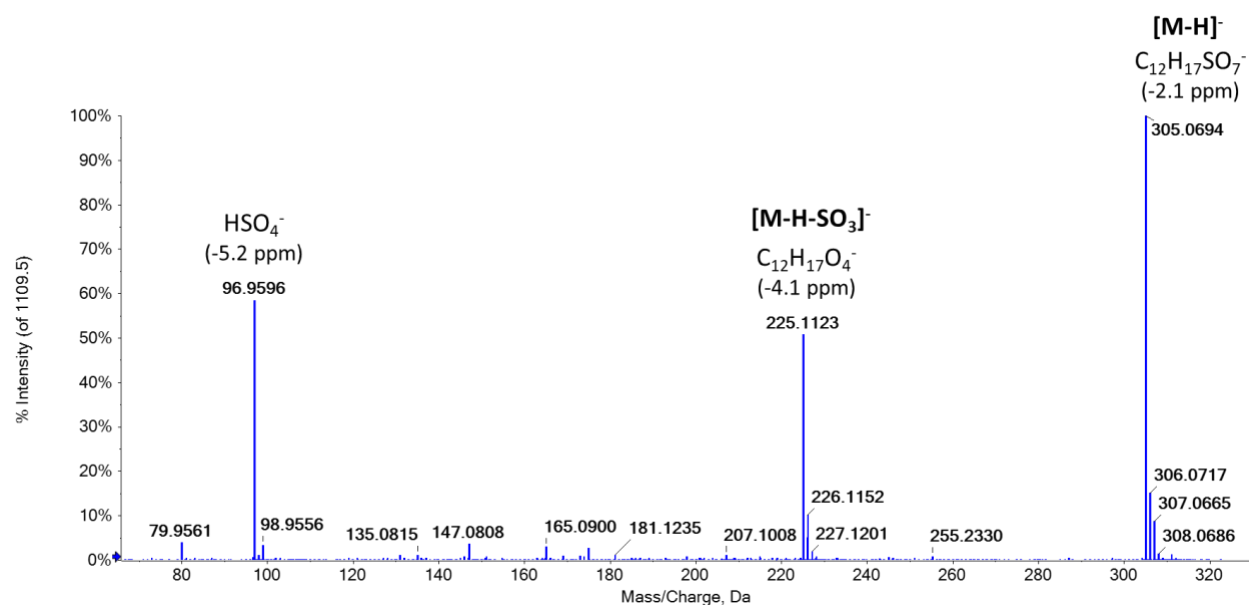


Figure S7-1. Tandem mass spectrum of m/z 305.0996 at t_R 3.5 min of compound **2**, annotated in methanolic root extract of *Lumnitzera littorea*. The spectrum was acquired with a QqTOF mass spectrometer operated in the negative SWATH mode (m/z window 289.0–315.0).

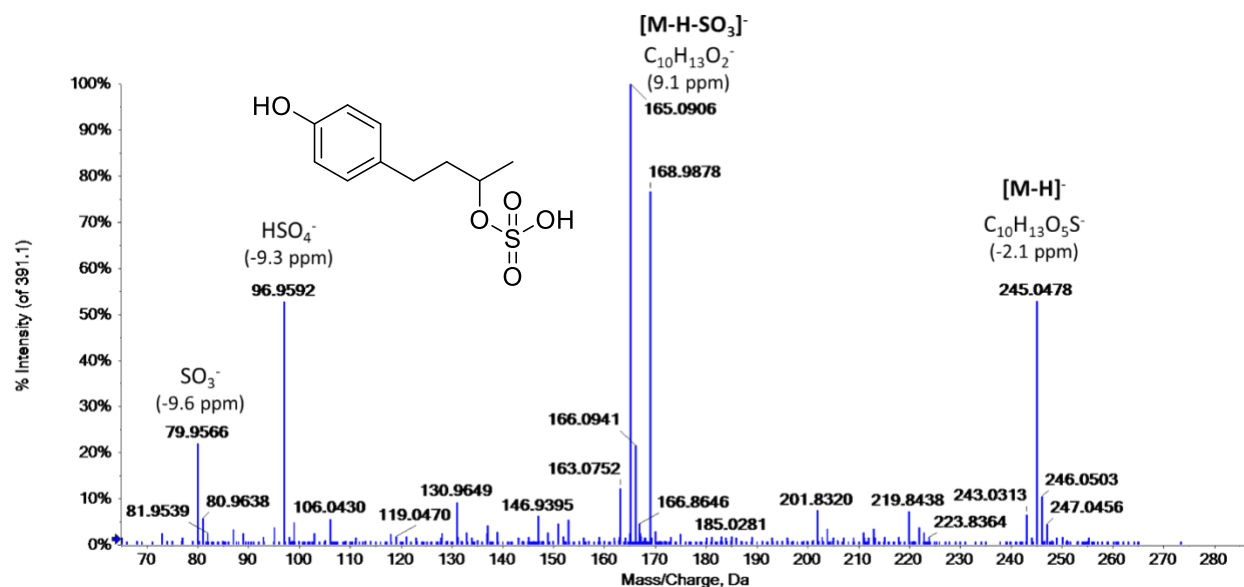


Figure S7-2. Tandem mass spectrum of m/z 245.0488 at t_R 3.8 min of compound **3**, annotated in methanolic root extracts of *Lumnitzera littorea* and *L. racemosa*. The spectrum was acquired with a QqTOF mass spectrometer operated in the negative SWATH mode (m/z window 239.0–265.0).

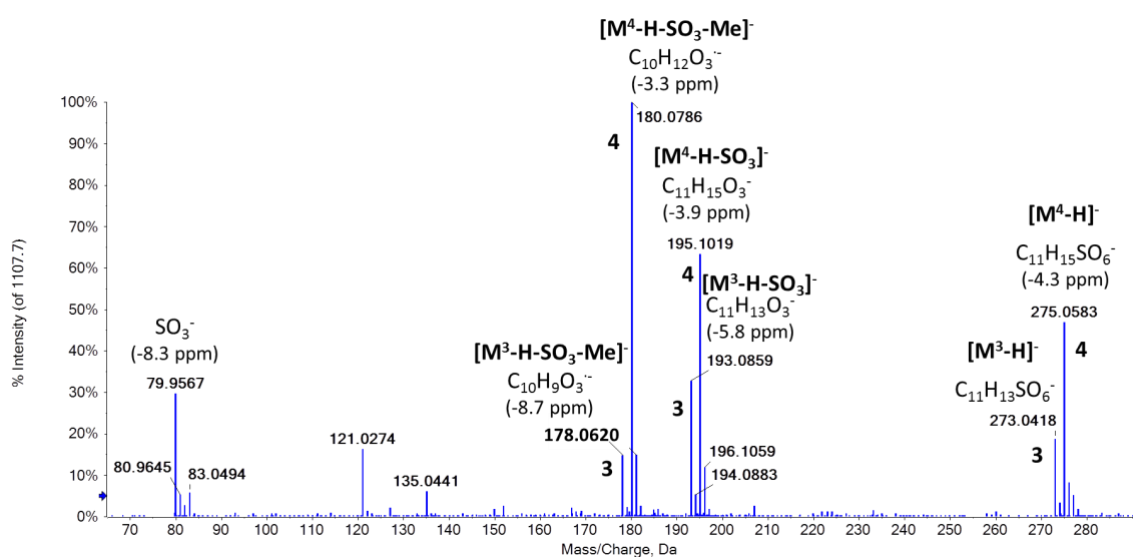


Figure S7-3. Tandem mass spectrum of m/z 273.0436 and 275.0591 at t_R 3.9 min of overlapping compounds **4** and **5**, respectively, annotated in methanolic root extracts of *Lumnitzera littorea* and *L. racemosa*. The spectrum was acquired with a QqTOF mass spectrometer operated in the negative SWATH mode (m/z window 264.0–290.0).

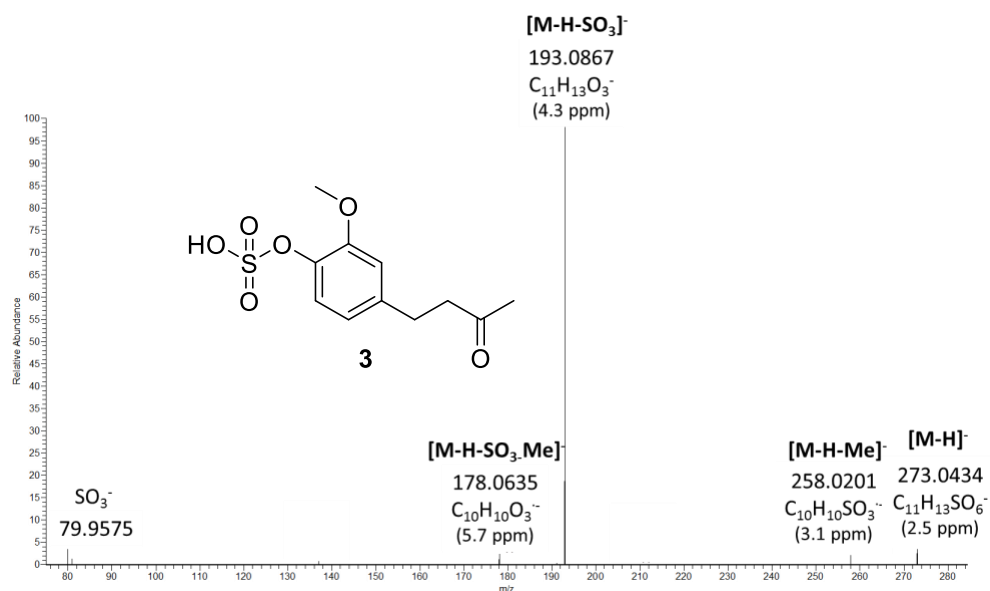


Figure S7-4. Tandem mass spectrum of m/z 273.0436 at t_R 3.9 min of compound **4**, annotated in methanolic root extracts of *Lumnitzera littorea* and *L. racemosa*. The spectrum was acquired with LIT-Orbitrap-MS in negative ion mode with CID activation (30% relative collision energy).

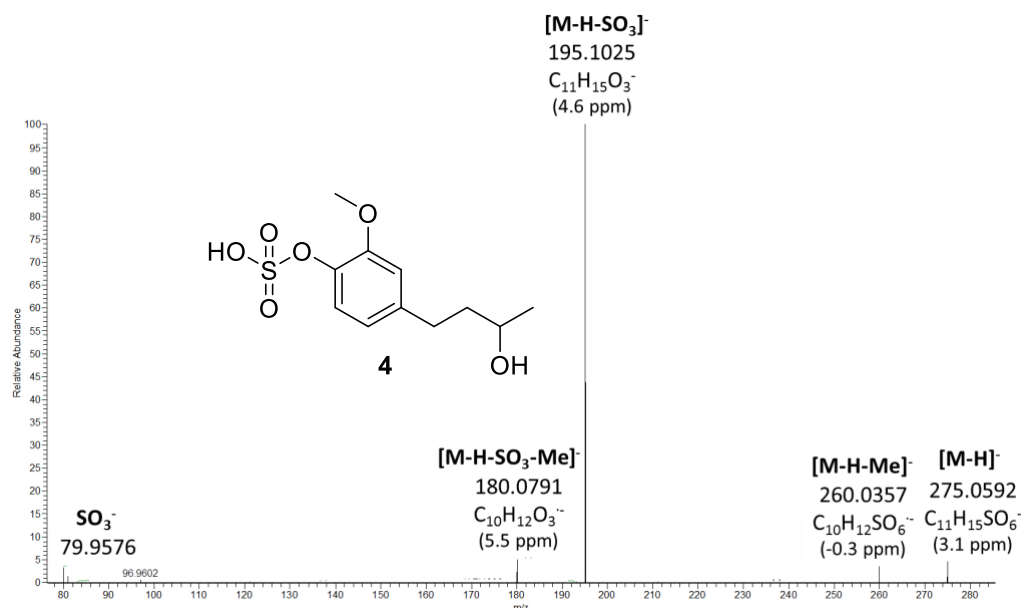


Figure S7-5. Tandem mass spectrum of m/z 275.0591 at t_R 3.9 min of compound **5**, annotated in methanolic root extracts of *Lumnitzera littorea* and *L. racemosa*. The spectrum was acquired with LIT-Orbitrap-MS in negative ion mode with CID activation (30% relative collision energy).

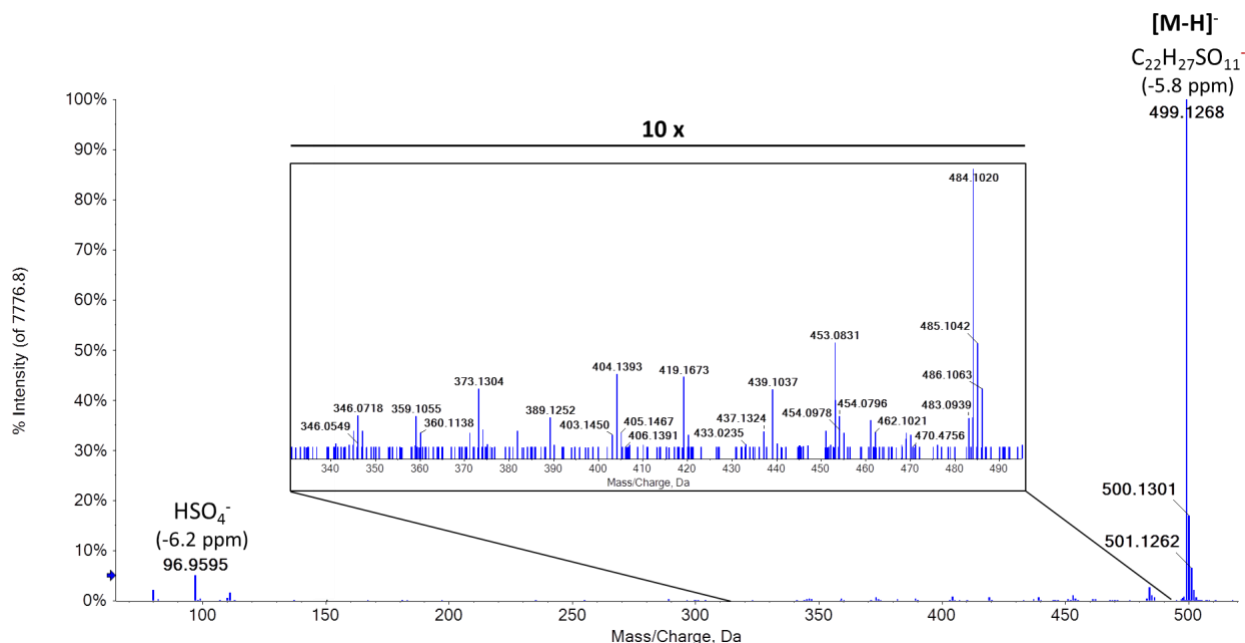


Figure S7-6. Tandem mass spectrum of m/z 499.1267 at t_R 4.4 min of compound **6**, annotated in methanolic root extracts of *Lumnitzera littorea*. The spectrum was acquired with a QqTOF mass spectrometer operated in the negative SWATH mode (m/z window 489.0–515.0).

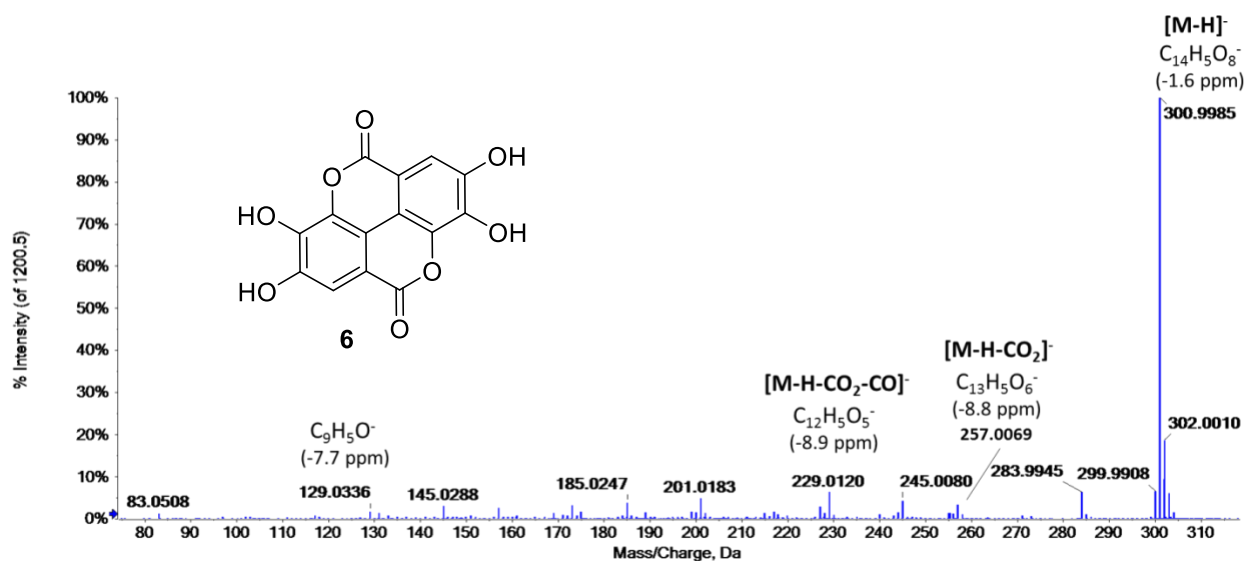


Figure S7-7. Tandem mass spectrum of m/z 300.9989 at t_R 4.4 min of compound **7**, annotated in methanolic root extracts of *Lumnitzera littorea*. The spectrum was acquired with a QqTOF mass spectrometer operated in the negative SWATH mode (m/z window 289.0–315.0).

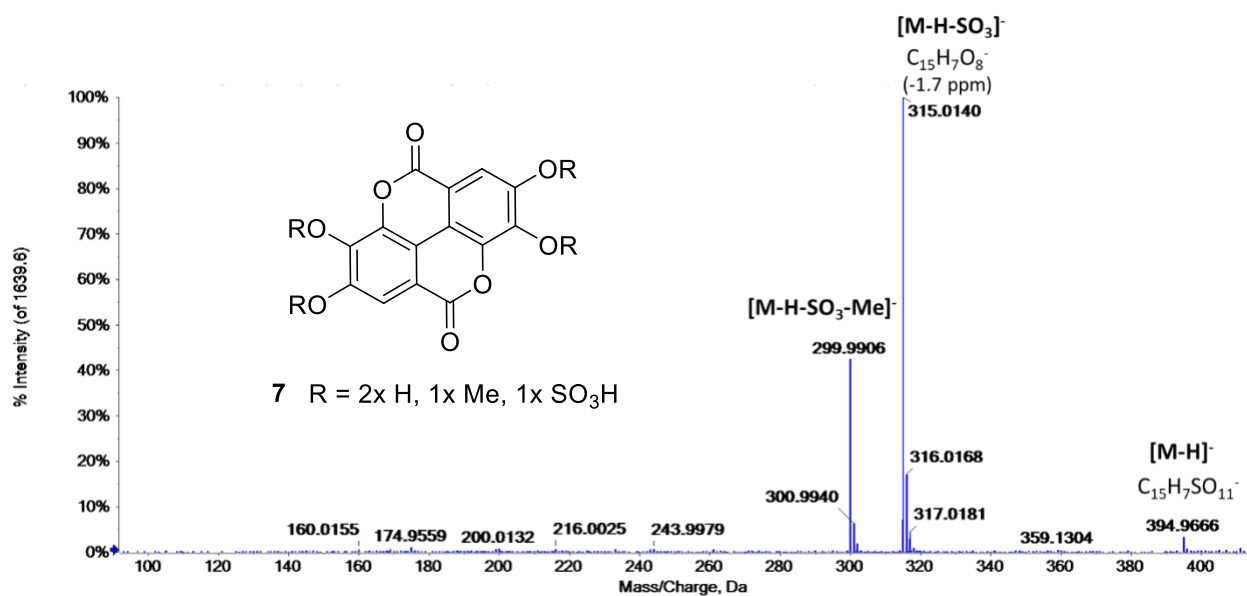


Figure S7-8. Tandem mass spectrum of m/z 394.9707 at t_R 5.3 min of compound **8**, annotated in methanolic root extracts of *Lumnitzera racemosa*. The spectrum was acquired with a QqTOF mass spectrometer operated in the negative SWATH mode (m/z window 389.0–415.0).

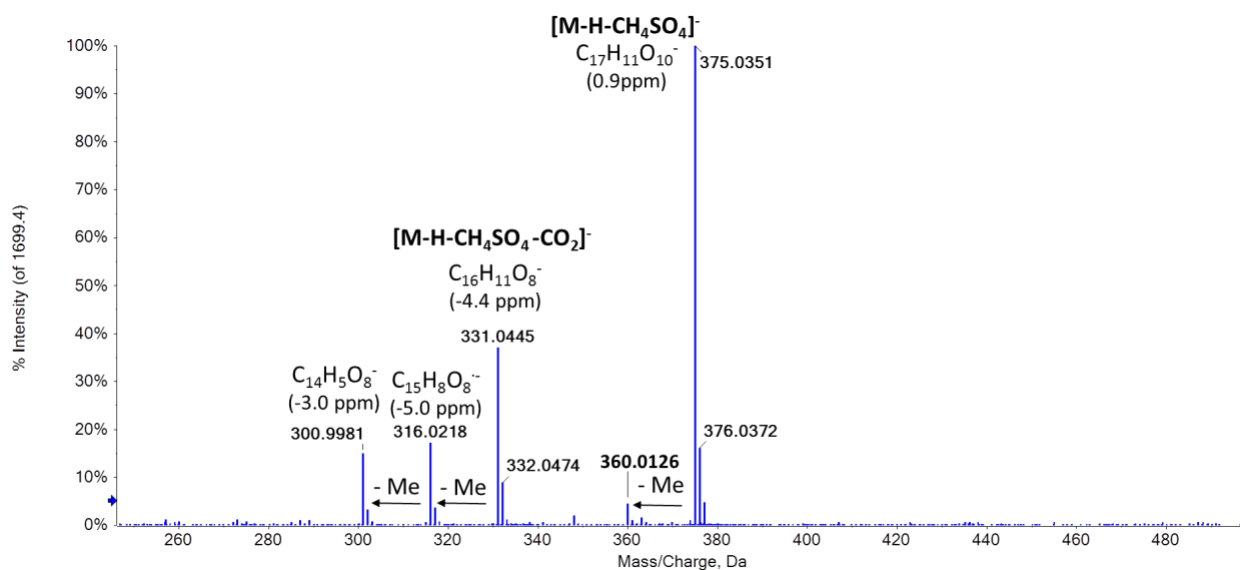


Figure S7-9. Tandem mass spectrum of m/z 487.0179 at t_R 5.5 min of compound **9**, annotated in the methanolic root extract of *Lumnitzera racemosa*. The spectrum was acquired with a QqTOF mass spectrometer operated in the negative SWATH mode (m/z window 464.0–490.0).

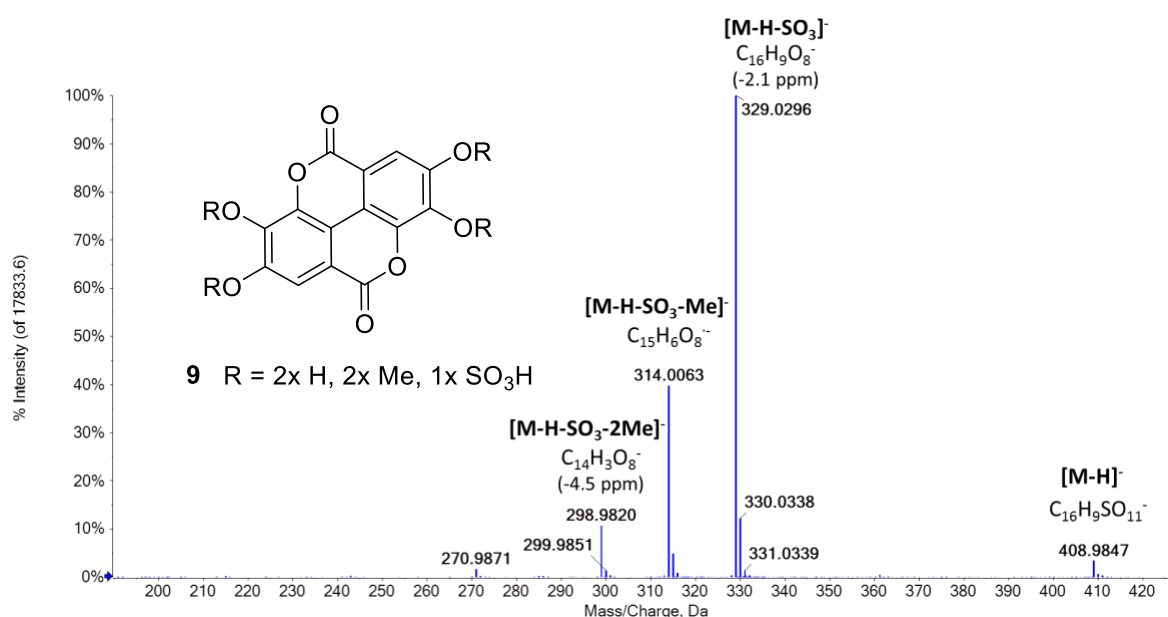


Figure S7-10. Tandem mass spectrum of m/z 408.9898 at t_R 5.7 min of compound **10**, annotated in methanolic root extracts of *Lumnitzera littorea* and *L. racemosa*. The spectrum was acquired with a QqTOF mass spectrometer operated in the negative SWATH mode (m/z window 389.0–415.0).

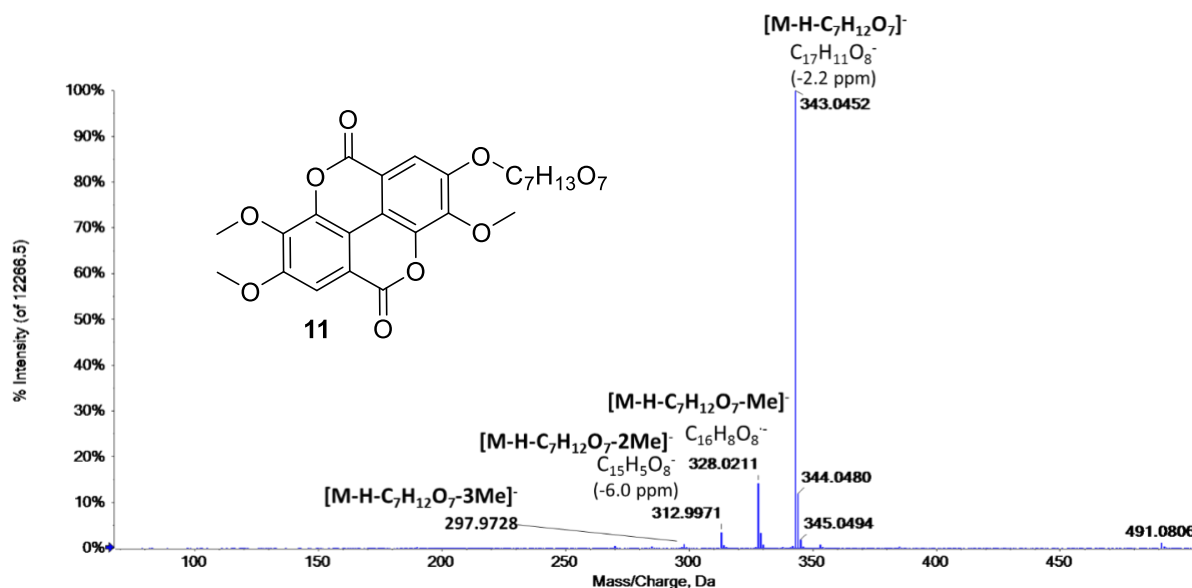


Figure S7-11. Tandem mass spectrum of m/z 551.1027 at t_R 6.0 min of compound **11**, annotated in methanolic root extracts of *Lumnitzera racemosa*. The spectrum was acquired with a QqTOF mass spectrometer operated in the negative SWATH mode (m/z window 539.0–565.0).

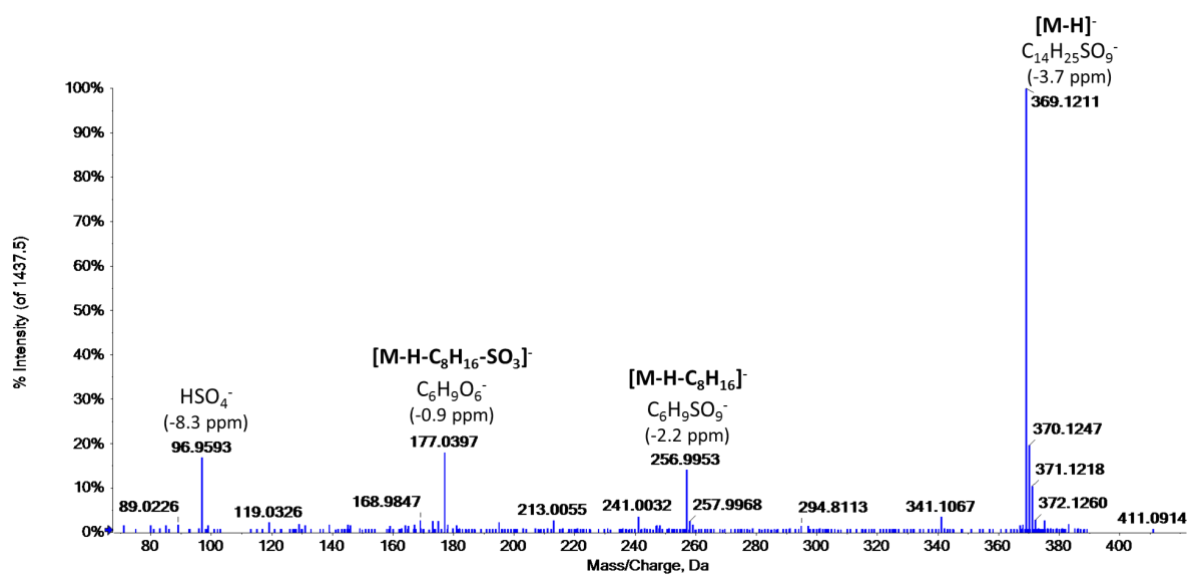


Figure S7-12. Tandem mass spectrum of m/z 369.1225 at t_R 6.1 min of compound **12**, annotated in methanolic root extracts of *Lumnitzera littorea*. The spectrum was acquired with a QqTOF mass spectrometer operated in the negative SWATH mode (m/z window 364.0–390.0).

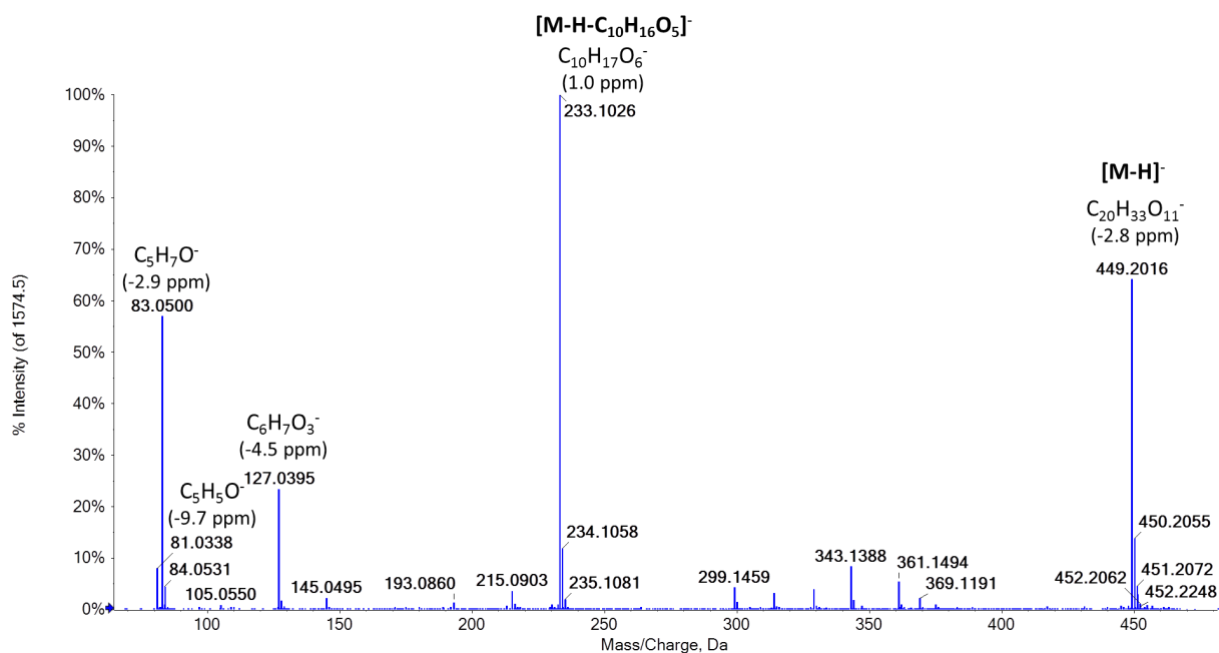


Figure S7-13. Tandem mass spectrum of m/z 449.2027 at t_R 6.3 min of compound **13**, annotated in methanolic root extracts of *Lumnitzera littorea* and *L. racemosa*. The spectrum was acquired with a QqTOF mass spectrometer operated in the negative SWATH mode (m/z window 439.0–465.0).

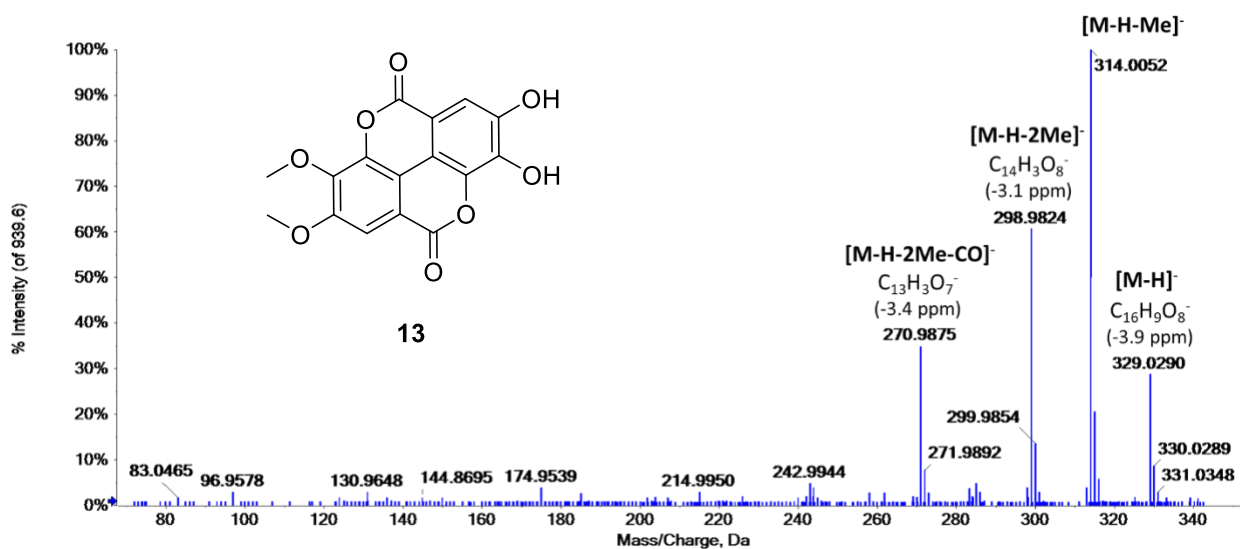


Figure S7-14. Tandem mass spectrum of m/z 329.0301 at t_R 6.4 min of compound **14**, annotated in methanolic root extracts of *Lumnitzera littorea* and *L. racemosa*. The spectrum was acquired with a QqTOF mass spectrometer operated in the negative SWATH mode (m/z window 314.0–340.0).

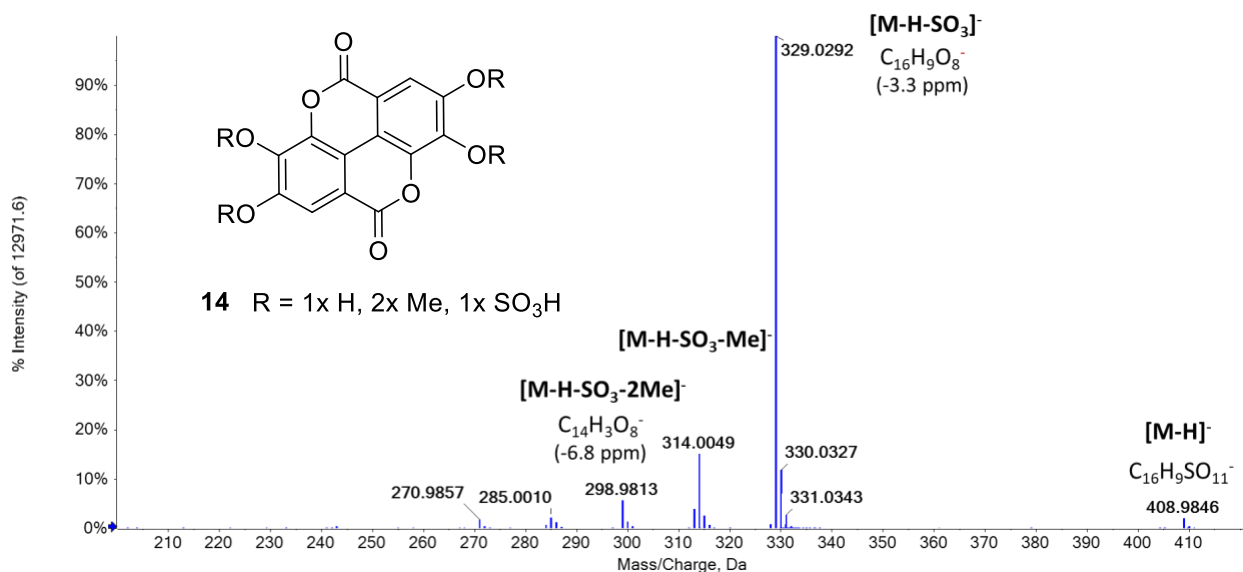


Figure S7-15. Tandem mass spectrum of m/z 408.9867 at t_R 6.5 min of compound **15**, annotated in methanolic root extracts of *Lumnitzera racemosa*. The spectrum was acquired with a QqTOF mass spectrometer operated in the negative SWATH mode (m/z window 389.0–415.0).

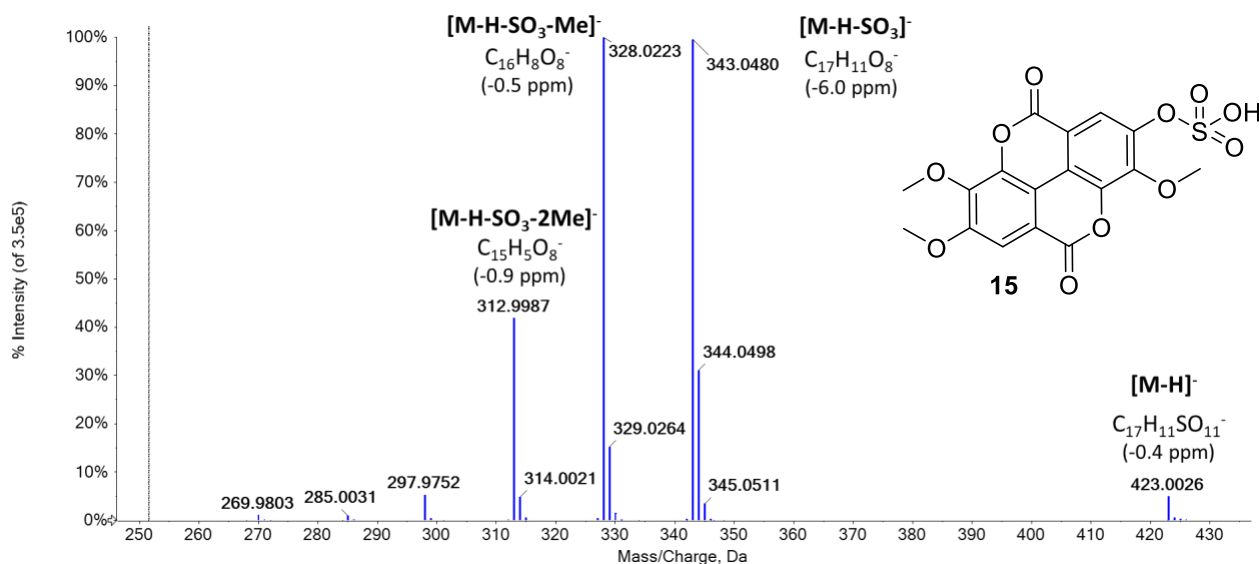


Figure S7-16. Tandem mass spectrum of m/z 423.0035 at t_R 6.9 min of compound **16**, annotated in methanolic root extracts of *Lumnitzera littorea* and *L. racemosa*. The spectrum was acquired with a QqTOF mass spectrometer operated in the negative SWATH mode (m/z window 414.0–440.0).

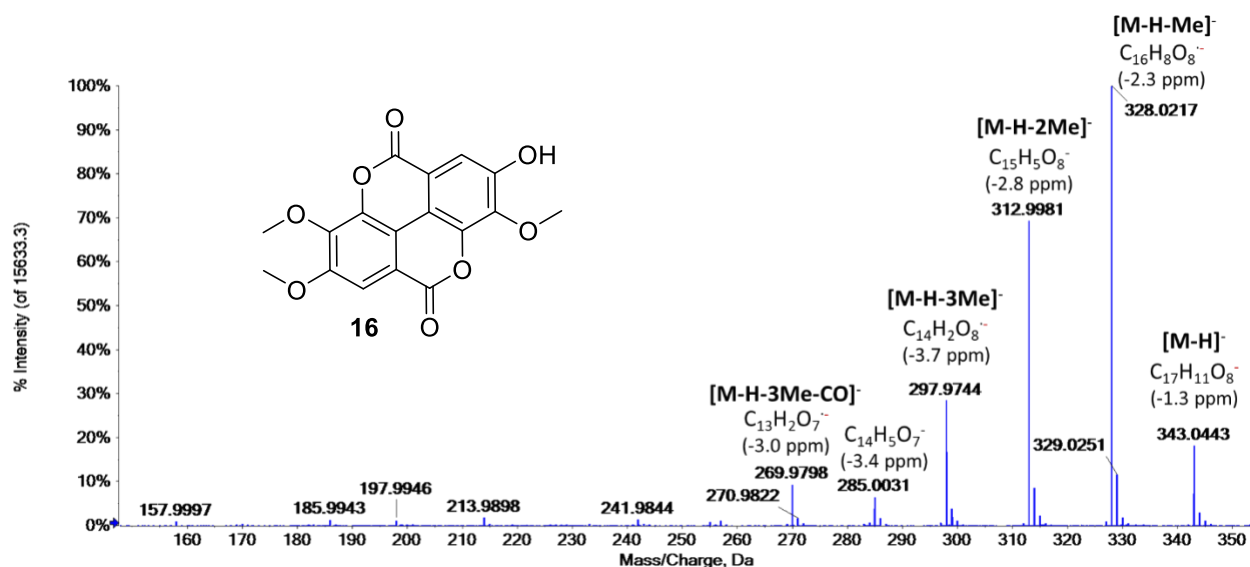


Figure S7-17. Tandem mass spectrum of m/z 343.0455 at t_R 7.7 min of compound **17**, annotated in methanolic root extracts of *Lumnitzera littorea* and *L. racemosa*. The spectrum was acquired with a QqTOF mass spectrometer operated in the negative SWATH mode (m/z window 339.0–365.0).

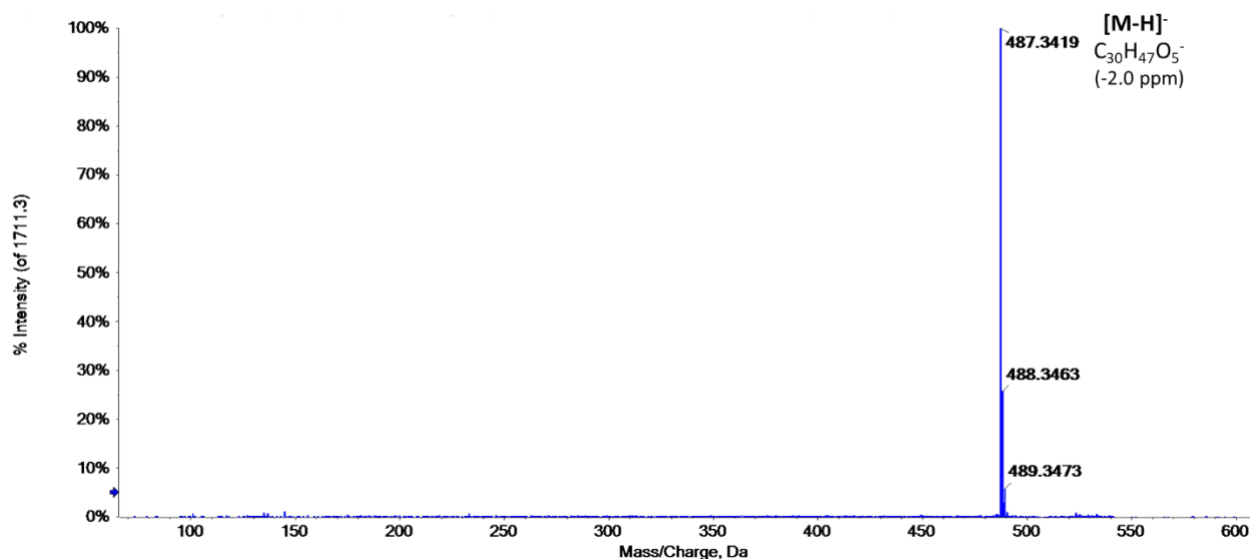


Figure S7-18. Tandem mass spectrum of m/z 533.3480 at t_R 9.8 min of the formiate adduct of compound **18**, annotated in methanolic root extracts of *Lumnitzera littorea* and *L. racemosa*. The spectrum was acquired with a QqTOF mass spectrometer operated in the negative SWATH mode (m/z window 514.0–540.0).

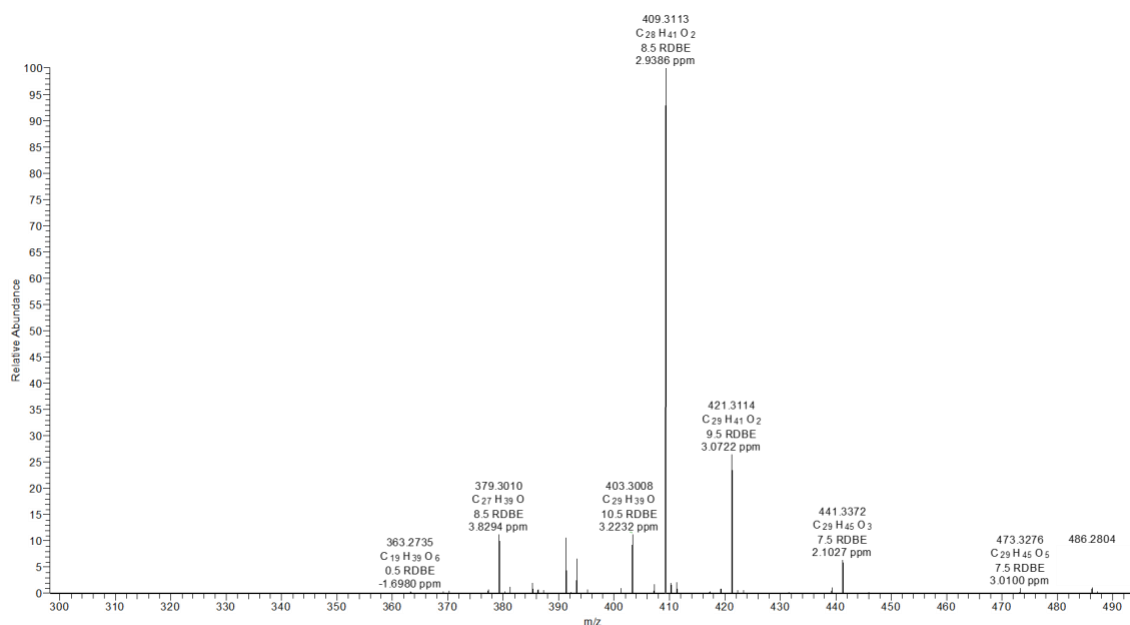


Figure S7-19. Tandem mass spectrum of m/z 487.3425 at t_R 9.8 min of compound **18**, annotated in methanolic root extracts of *Lumnitzera littorea* and *L. racemosa*. The spectrum was acquired with LIT-Orbitrap-MS in negative ion mode with CID activation (35% relative collision energy).

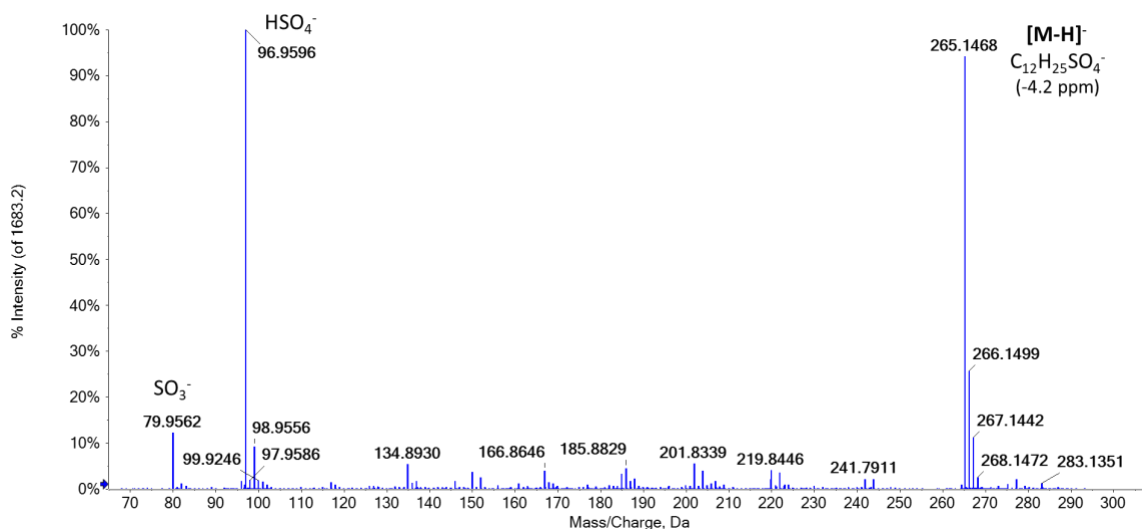


Figure S7-20. Tandem mass spectrum of m/z 265.1476 at t_R 12.2 min of compound **19**, annotated in methanolic root extracts of *Lumnitzera littorea* and *L. racemosa*. The spectrum was acquired with a QqTOF mass spectrometer operated in the negative SWATH mode (m/z window 264.0–290.0).

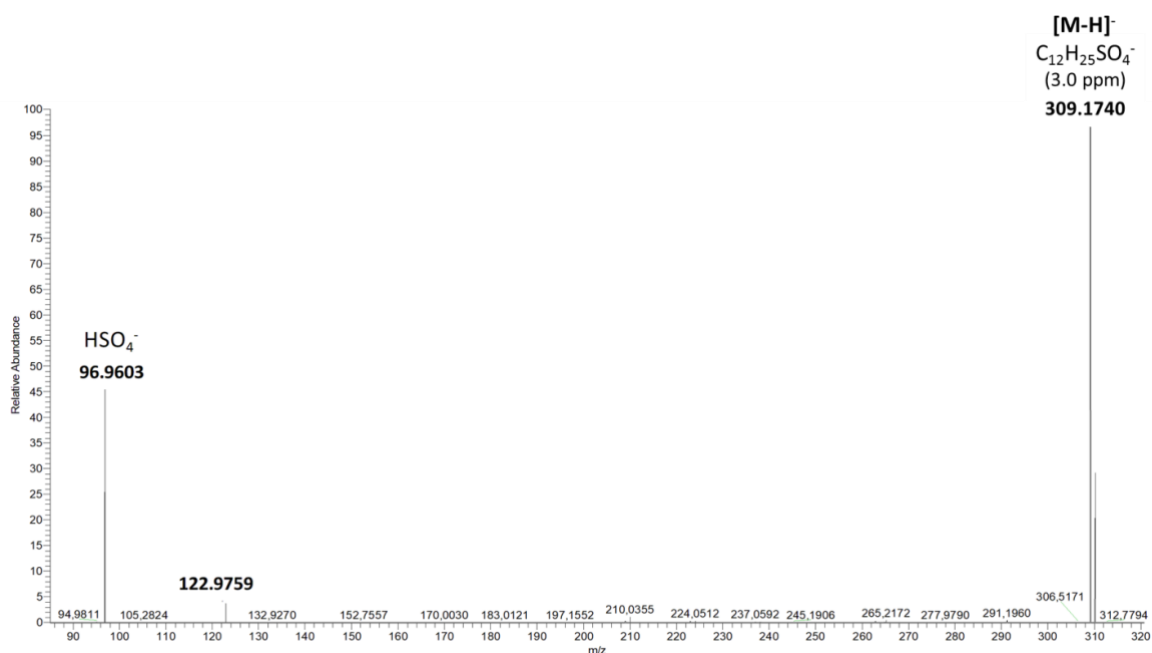


Figure S7-21. Tandem mass spectrum of m/z 309.1733 at t_R 13.4 min of compound **20**, annotated in methanolic root extracts of *L. littorea* and *L. racemosa*. The spectrum was acquired with LIT-Orbitrap-MS in negative ion mode with CID activation (35% relative collision energy).

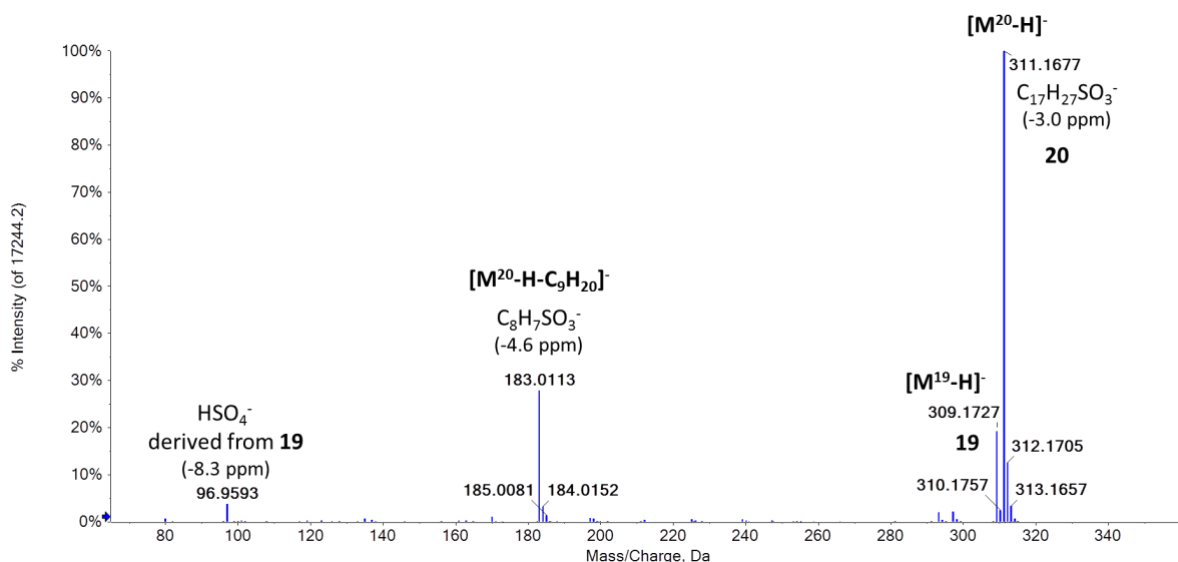


Figure S7-22. Tandem mass spectrum of m/z 309.1733 and 311.1685 at t_R 13.4 min of compounds **20** and **21**, respectively, annotated in methanolic root extracts of *Lumnitzera littorea* and *L. racemosa*. The spectrum was acquired with a QqTOF mass spectrometer operated in the negative SWATH mode (m/z window 289.0–315.0).

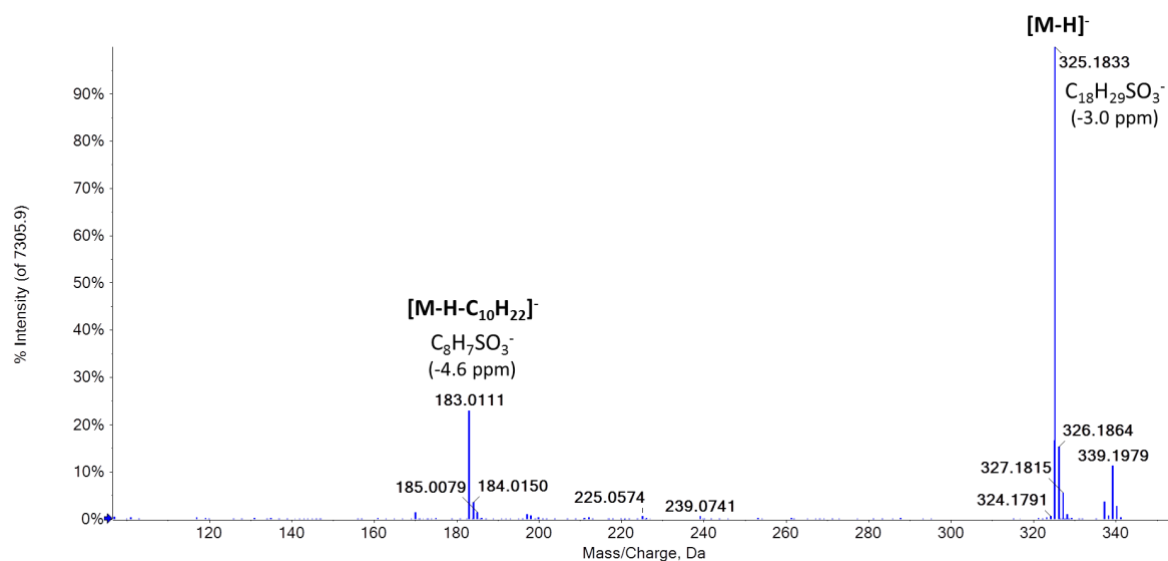


Figure S7-23. Tandem mass spectrum of m/z 325.1833 at t_R 14.6 min of compound **22**, annotated in methanolic root extracts of *Lumnitzera littorea* and *L. racemosa*. The spectrum was acquired with a QqTOF mass spectrometer operated in the negative SWATH mode (m/z window 314.0–340.0).

Table S5. Peak areas (presented as counts per second) of main compounds integrated in total ion chromatograms (TIC) acquired for root extracts of *Lumnitzera littorea* (1-13) and *L. racemosa* (15-35) by UHPLC-ESI-Q-MS.

Compound	2	4	3	6	7	9	10	13	15	16
rt (min)	2,5	2,55	2,6	2,8	3,25	3,5	3,7	4.0	4,2	4,8
m/z	245	275	273	301	395	409	551	329	423	343
1	16305					6238			110995	16608
2	no results									
3	13630			1513		122511			114942	22498
4	24579					4649			88144	22967
7	no results									
12	no results									
9				6535		5462			106017	36740
13	3789					1057		2670	40123	37841
11	21145					9796			151009	23011
10	25221		4150			16614			198140	40378
6		3748		2550	12559	28413	2299		151567	13810
8	6384					3478			149719	26341
16	no results									
15			78929	4551		56839		18648	-	-
15	2505	1491		5236	3122	122511		19629	-	-
18			79472	7763		138091		40885	-	-
22		15620	14988	10647	2798	6100	15731	1745	109580	33141
32	no results									
33		81480		51234		1907		51480	169288	159443
35			53366			129533		192405	-	-
30	2960		36775	12512			19070		104486	18387
17		5159		7683	2742	62649	4764	38071	268823	176536
27			51202	8262		5296	19239		89767	trace
28		12224	14599	2868	3528	13273	15569		135585	13301
29			24944			34692	14871	5170	321378	43682
26		73803				8577	15843		103275	12378
23		12486			37950	13877	58091		253222	64018
24				6150		3113	5317		151301	30436
25		9662	29179	6747	8754	52981	22757		193709	18905
20	15725		58754	12312	8944	27402	17967		340237	42964
19		22624	22765			8366	8810		224365	9920

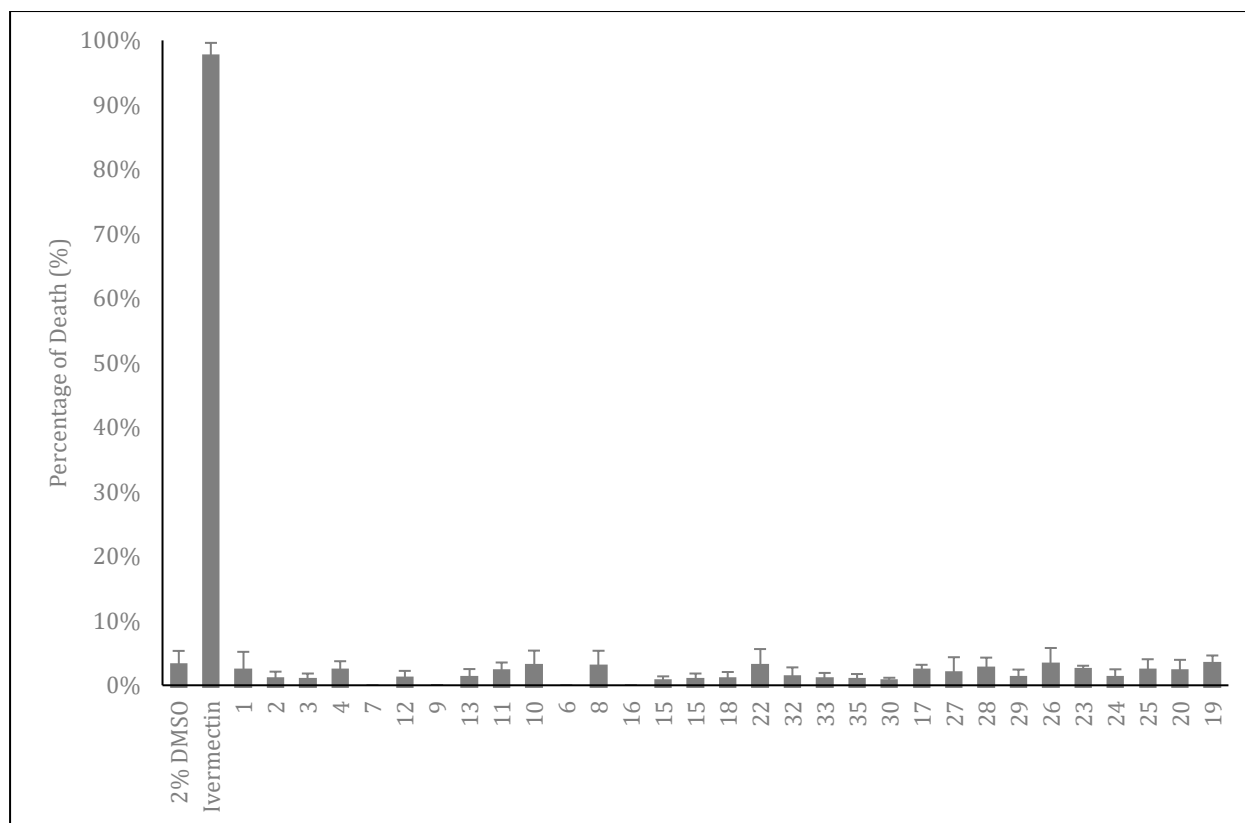
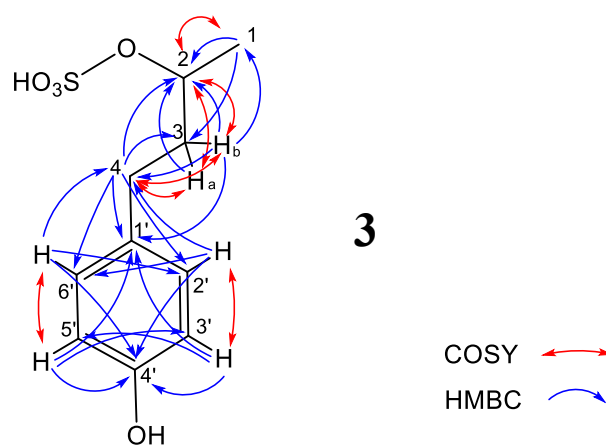


Figure S8. Anthelmintic activity of root extracts from *Lumnitzera littorea* (1-13) and *L. racemosa* (15-35) at the concentration of 500 $\mu\text{g}/\text{ml}$ against *Caenorhabditis elegans*. The solvent DMSO (2% v/v) and the standard anthelmintic drug ivermectin (10 $\mu\text{g}/\text{mL}$, 100% dead worms after 30 min incubation) were used as negative and positive controls, respectively. Results are given as percentage of dead worms.

Table S6. NMR spectroscopic data (400 MHz, methanol-d4) for 4-(4-hydroxyphenyl)-2-butanol 2-*O*-sulfate (**3**).

position	δ_C^a , type	δ_H (J in Hz)	COSY	HMBC
1	21.2, CH ₃	1.33, d (6.3)	2	2, 3
2	76.8, CH	4.46, m	1, 3a,b	
3	40.5, CH ₂	1.89 (3a), m	2, 4	2
		1.75 (3b), m		1, 2, 4, 1'
4	31.8, CH ₂	2.55-2.70, m	3a,b	2, 3, 1', 2', 6'
1'	134.6 ^b , C			
2'	130.3, CH	7.03, d-like (8.4)	3'	4, 4', 6'
3'	116.1, CH	6.67, d-like (8.4)	2	1', 4', 5'
4'	156.4 ^b , C			
5'	116.1, CH	6.67, d-like (8.4)	6'	1', 3', 4'
6'	130.3, CH	7.03, d-like (8.4)	5'	4, 2', 4'

^a derived from HSQC or ^b HMBC



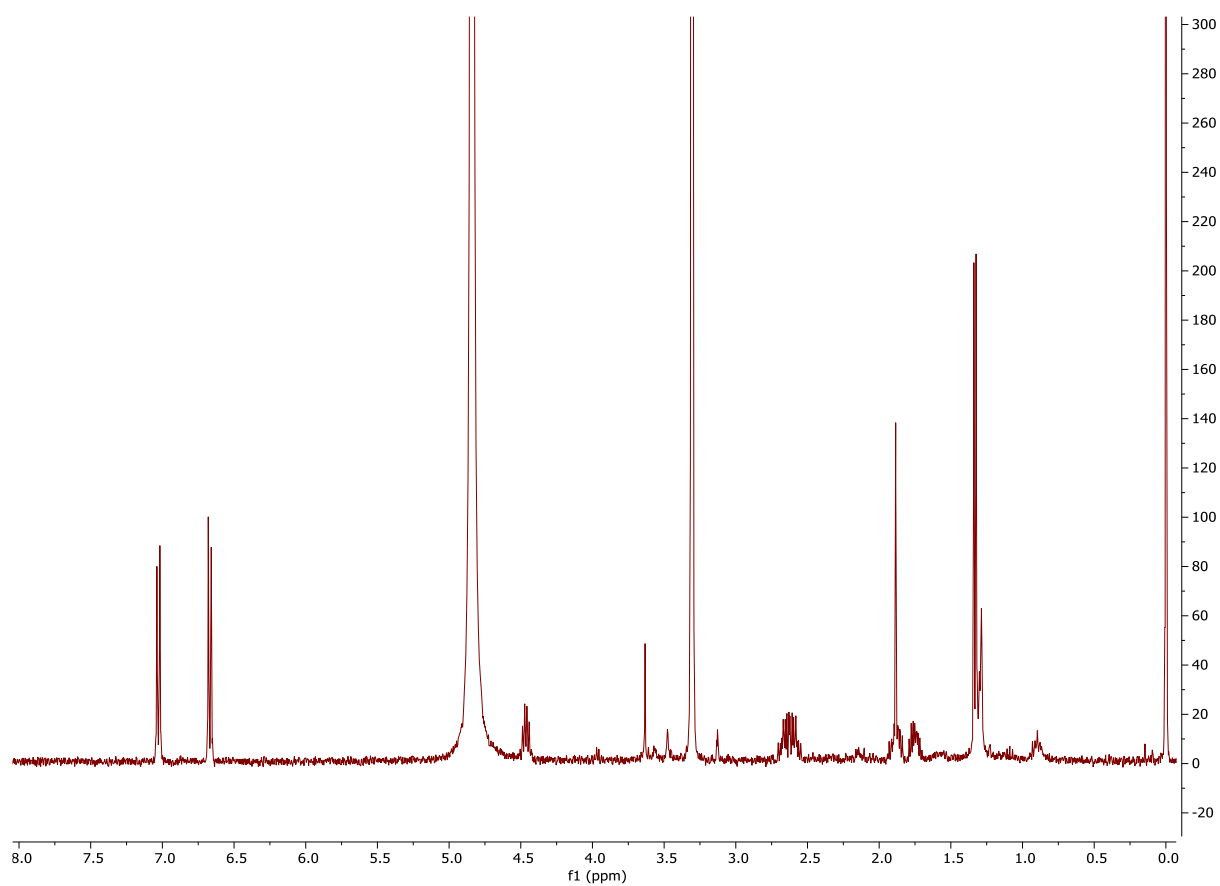


Figure S9-1. ^1H NMR spectrum of 4-(4-hydroxyphenyl)-2-butanol 2-*O*-sulfate (**3**).

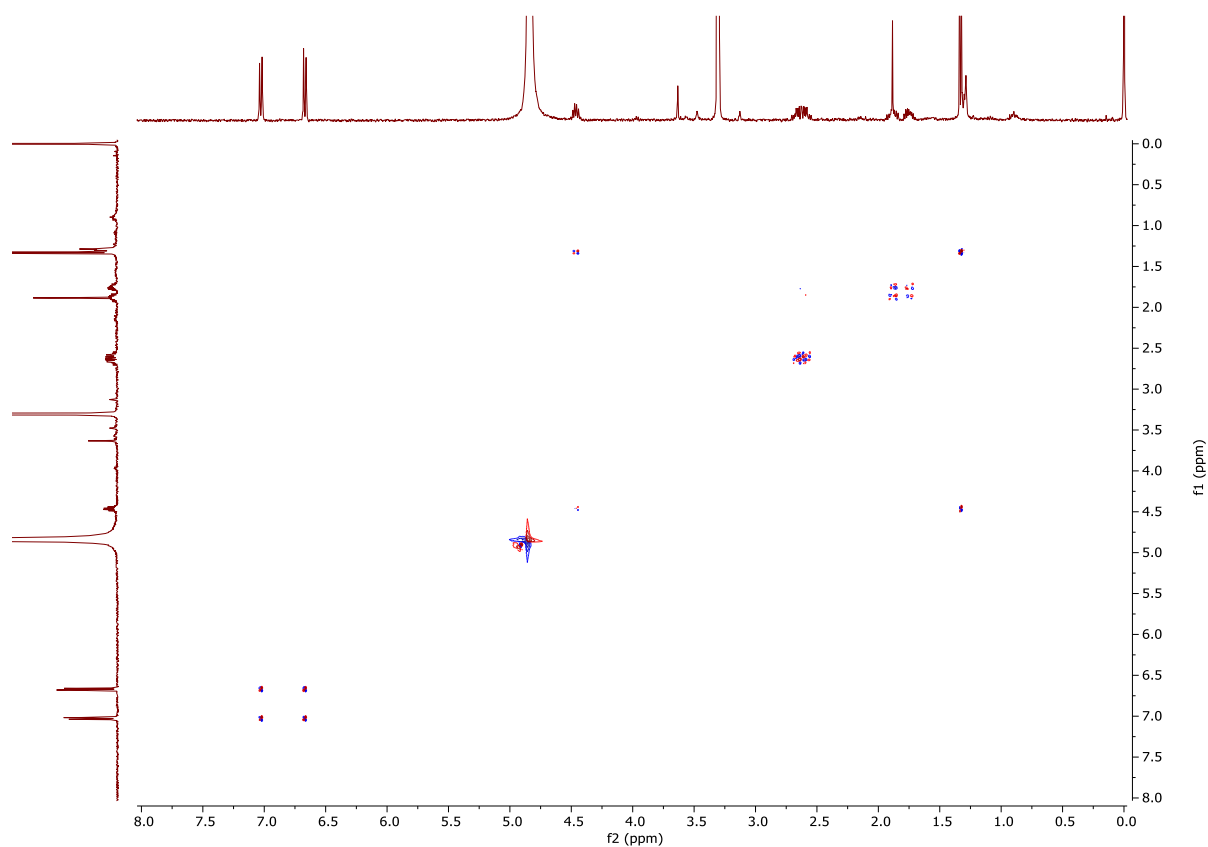
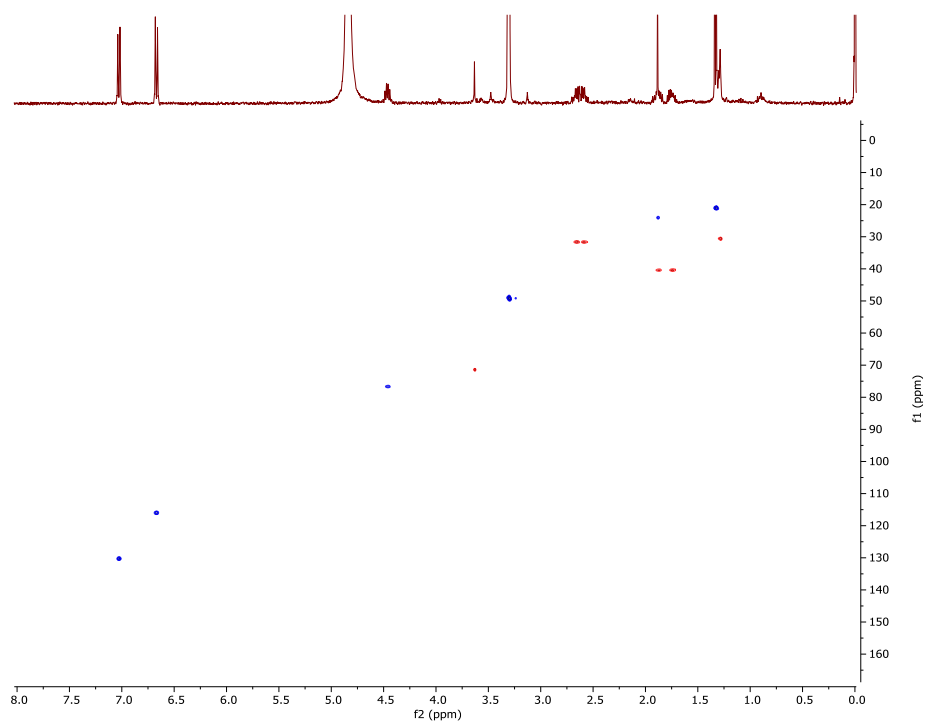
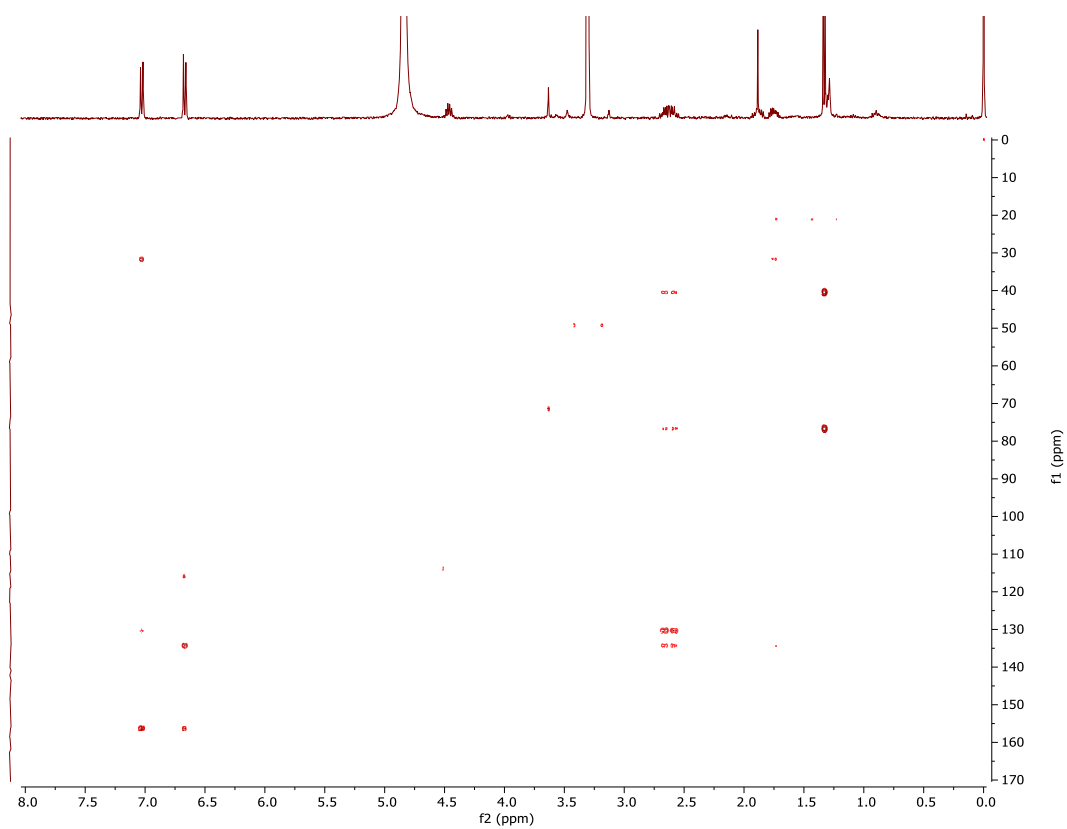


Figure S9-2. COSY spectrum of 4-(4-hydroxyphenyl)-2-butanol 2-*O*-sulfate (**3**).**Figure S9-3.** HSQC spectrum of 4-(4-hydroxyphenyl)-2-butanol 2-*O*-sulfate (**3**).**Figure S9-4.** HMBC spectrum of 4-(4-hydroxyphenyl)-2-butanol 2-*O*-sulfate (**3**).

KAJ008 I-S2+HPLCII nMS2-3#139-261 RT: 4.14-5.32 AV: 25 NL: 8.39E6
T: FTMS - p ESI Fullms [120.00-1000.00]

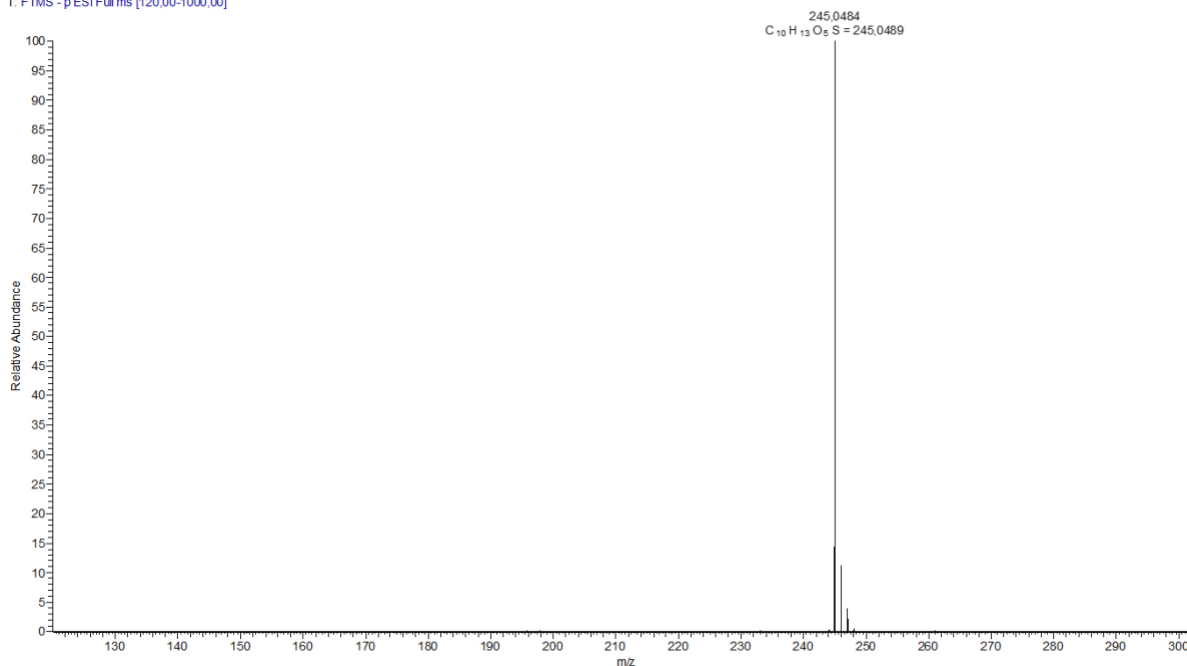


Figure S9-5. Full HRMS spectrum of 4-(4-hydroxyphenyl)-2-butanol 2-*O*-sulfate (**3**) acquired with LIT-Orbitrap-MS in negative ion mode.

KAJ008 I-S2+HPLCIII nMS2-3#128-273 RT: 3.79-5.39 AV: 29 NL: 3.35E3
F: FTMS - c ESI Fullms3 245.00@cid30.00 165.00@cid30.00 [50.00-250.00]

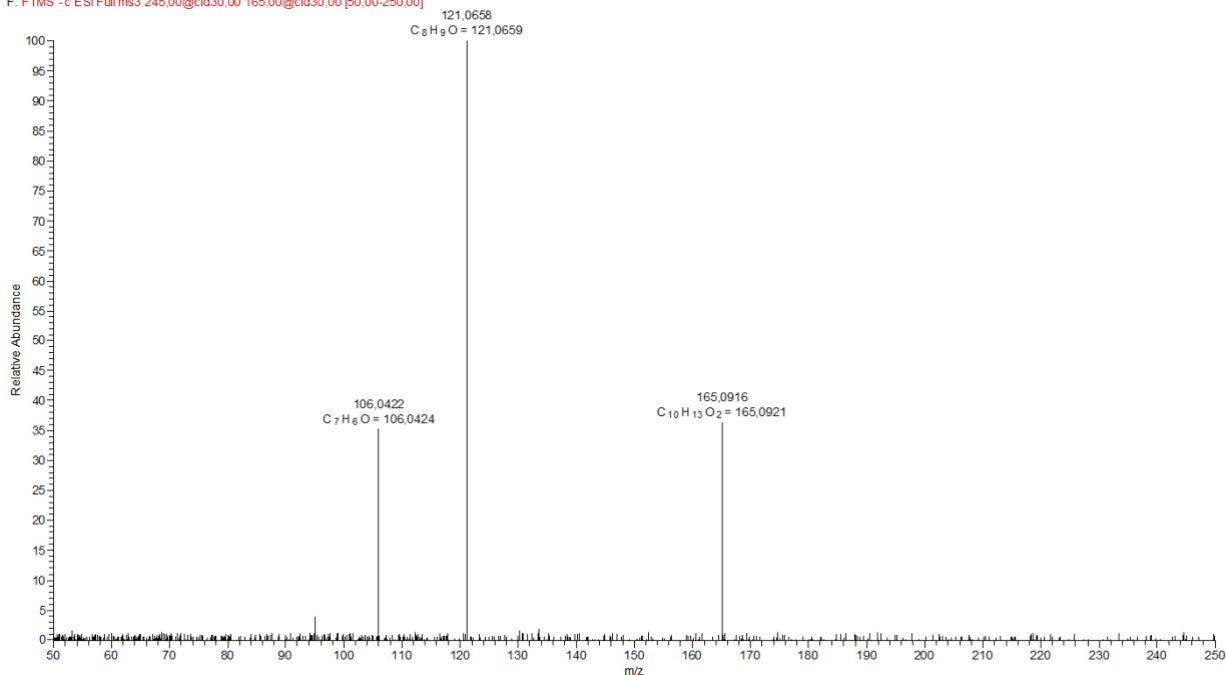
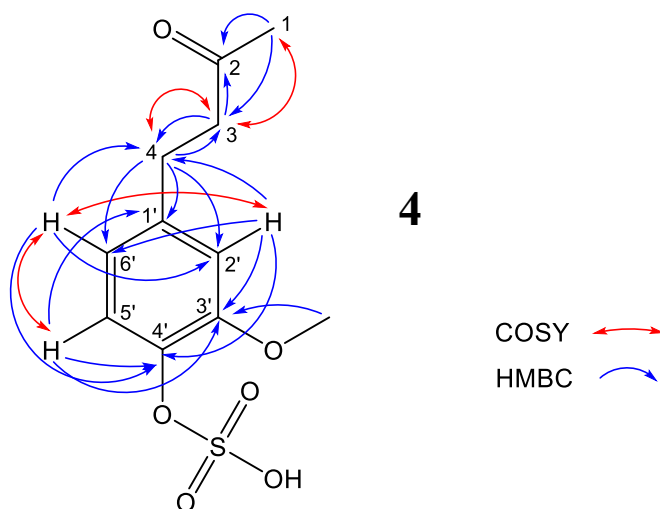


Figure S9-6. MS2 spectrum of 4-(4-hydroxyphenyl)-2-butanol 2-*O*-sulfate (**3**) acquired with LIT-Orbitrap-MS in negative ion mode with CID activation (30% relative collision energy).

Table S7. NMR spectroscopic data (400 MHz, methanol-d4) for 4-(4-sulfoxy-3-methoxyphenyl)-butan-2-one (**4**).

position	δ_c , type	δ_H (J in Hz)	COSY	HMBC
1	30.06, CH ₃	2.11, s	3	2, 3
2	211.47, C=O			
3	46.30, CH ₂	2.76, s	1, 4	2, 4
4	30.55, CH ₂	2.76, s	3	3, 1', 2', 6'
1'	134.02, C			
2'	113.14, CH	6.77, d (2.0)	6'	4, 3', 4', 6'
3'	148.96, C	-		
4'	145.85, C	-		
5'	116.20, CH	6.68, d (8.0)	6'	1', 3', 4',
6'	121.70, CH	6.61, dd (8.0, 2.0)	2', 5'	4, 2', 4'
3'-OMe	56.39, CH ₃	3.82, s		3'



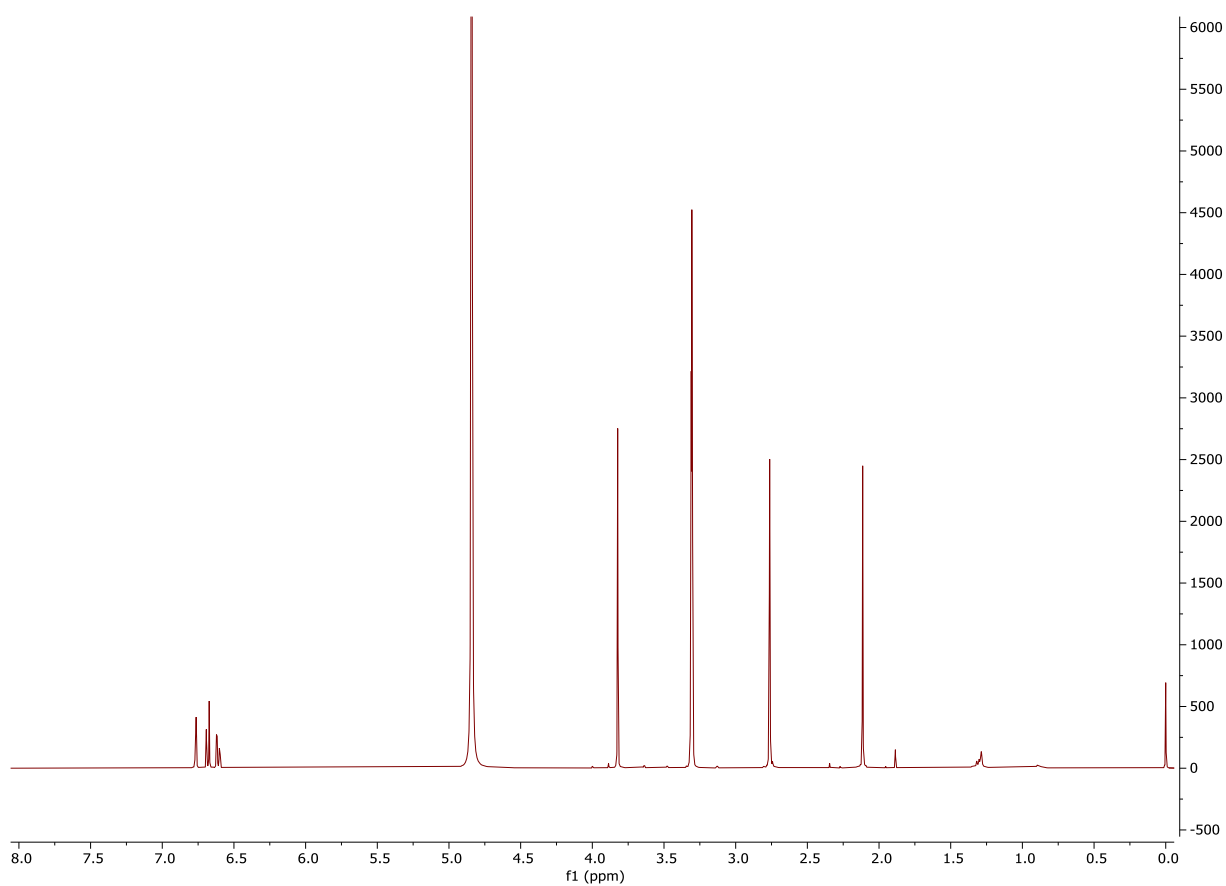


Figure S10-1. ¹H NMR spectrum of 4-(4-sulfoxy-3-methoxyphenyl)-butan-2-one (**4**).

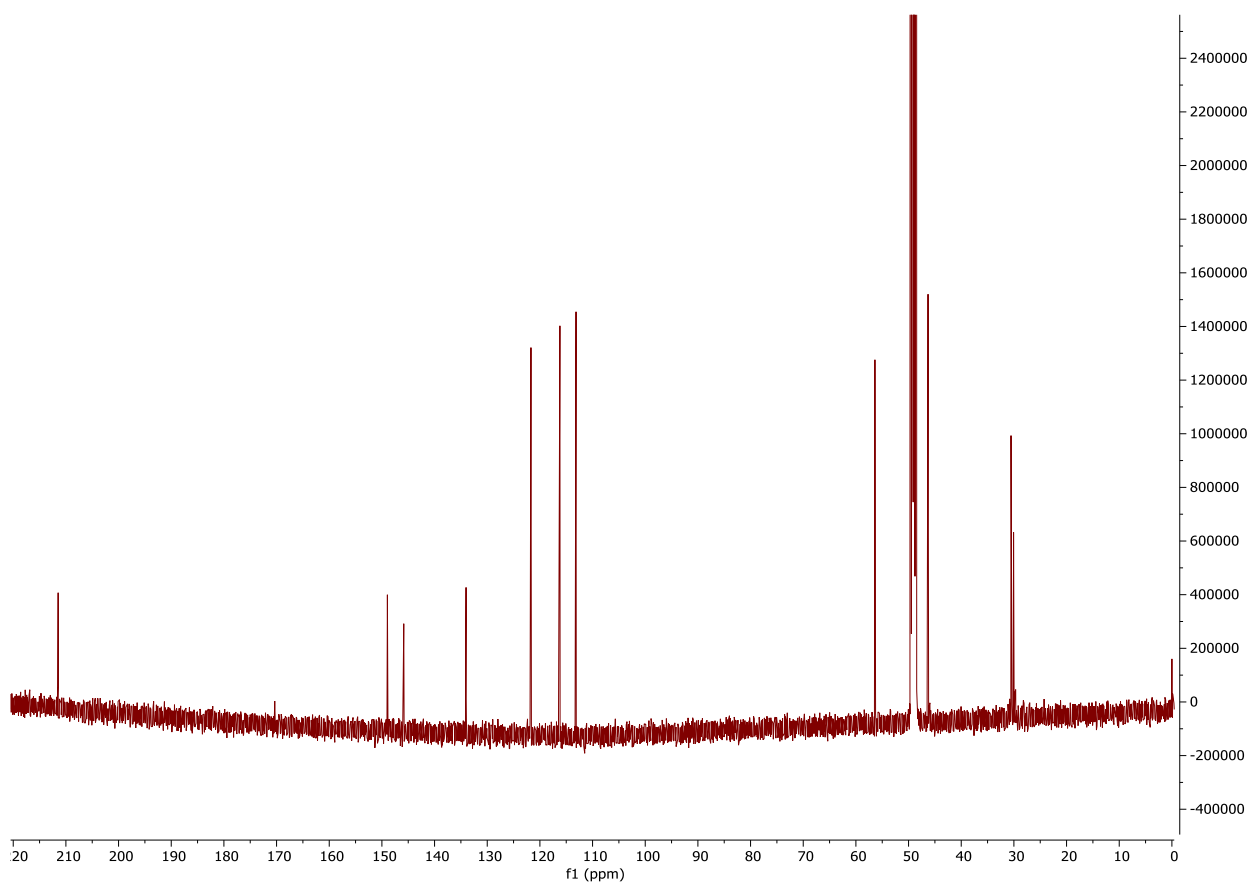


Figure S10-2. ¹³C NMR spectrum of 4-(4-sulfoxy-3-methoxyphenyl)-butan-2-one (**4**).

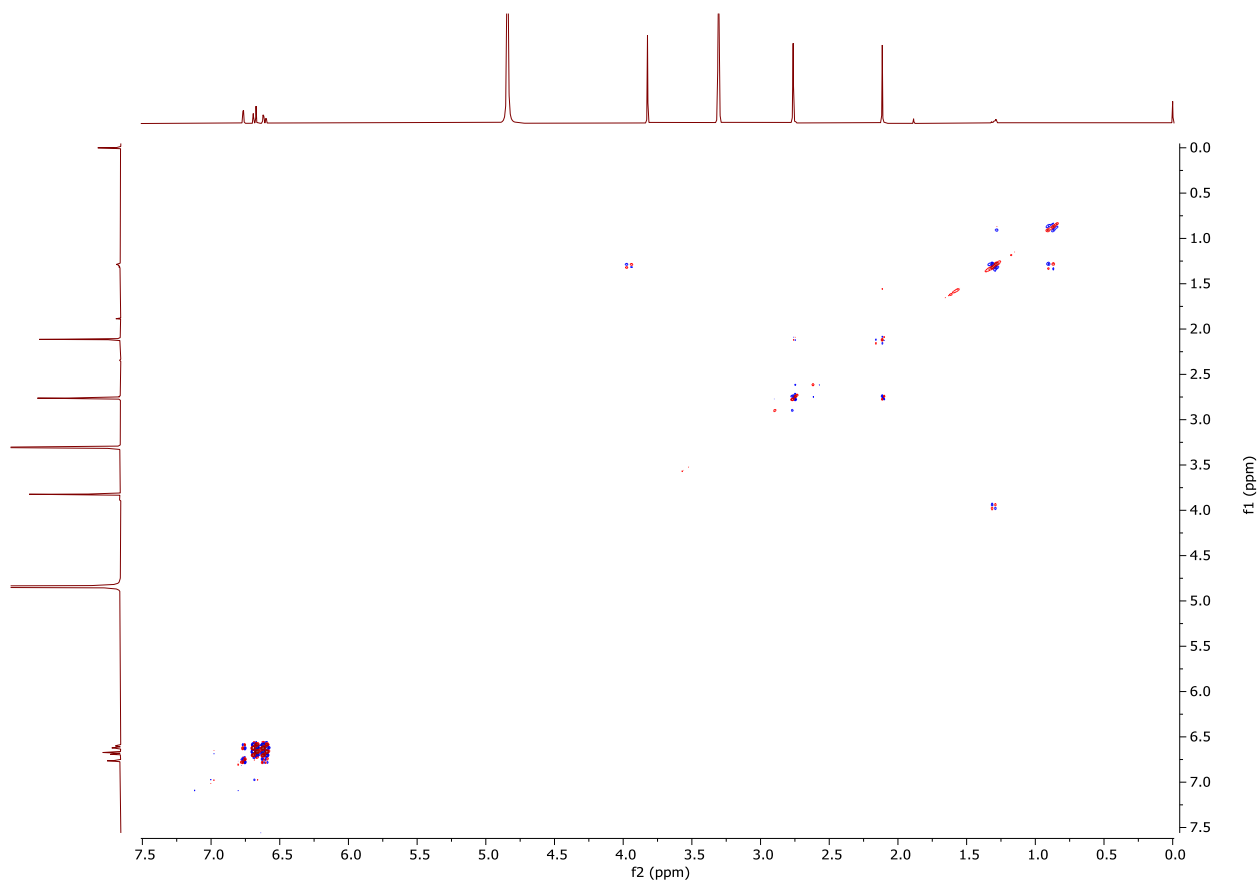


Figure S10-3. COSY spectrum of 4-(4-sulfoxy-3-methoxyphenyl)-butan-2-one (**4**).

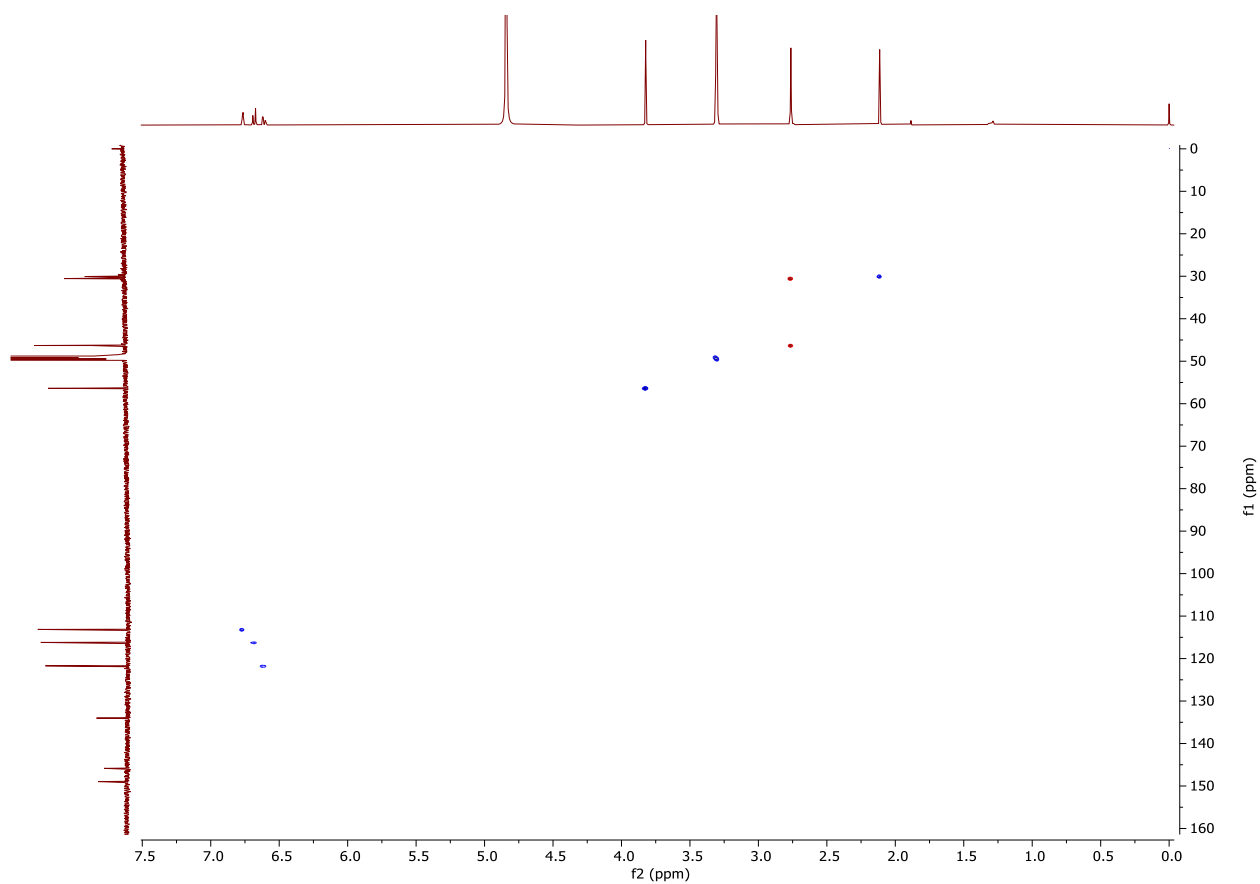
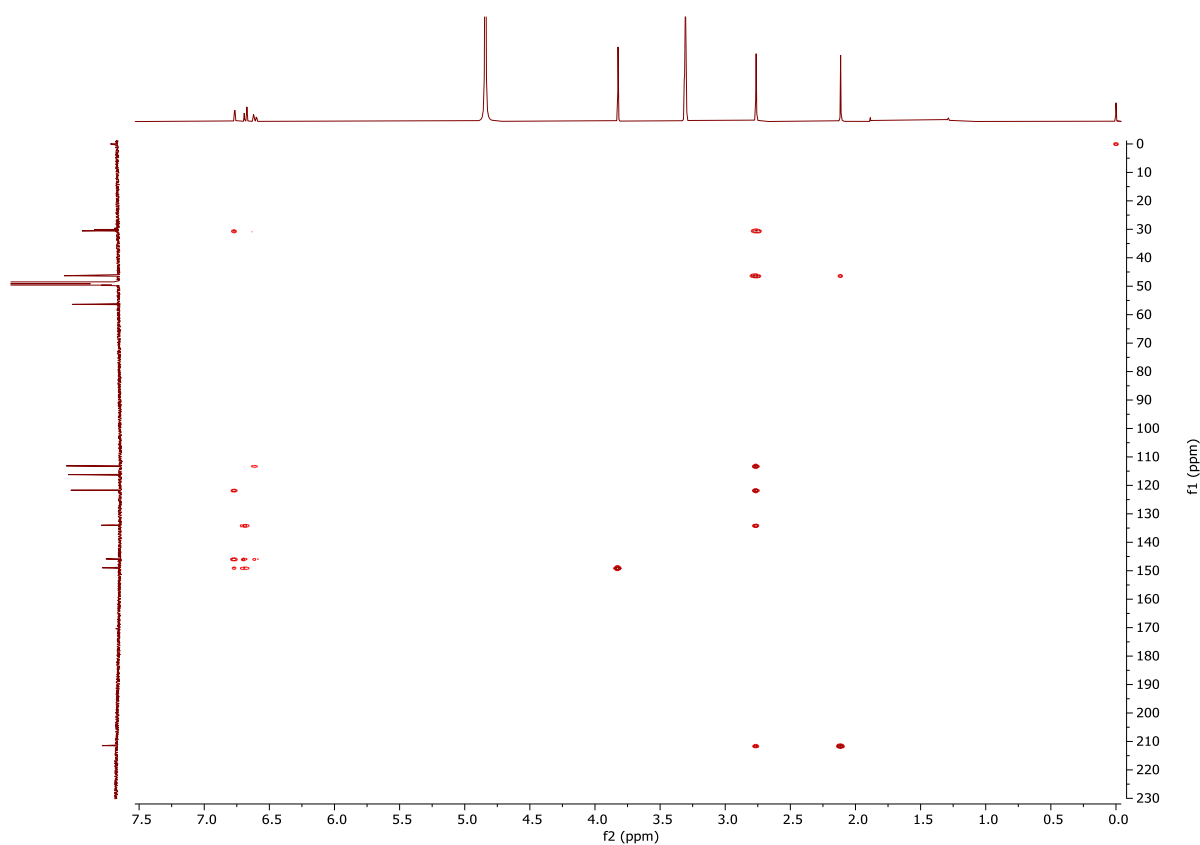
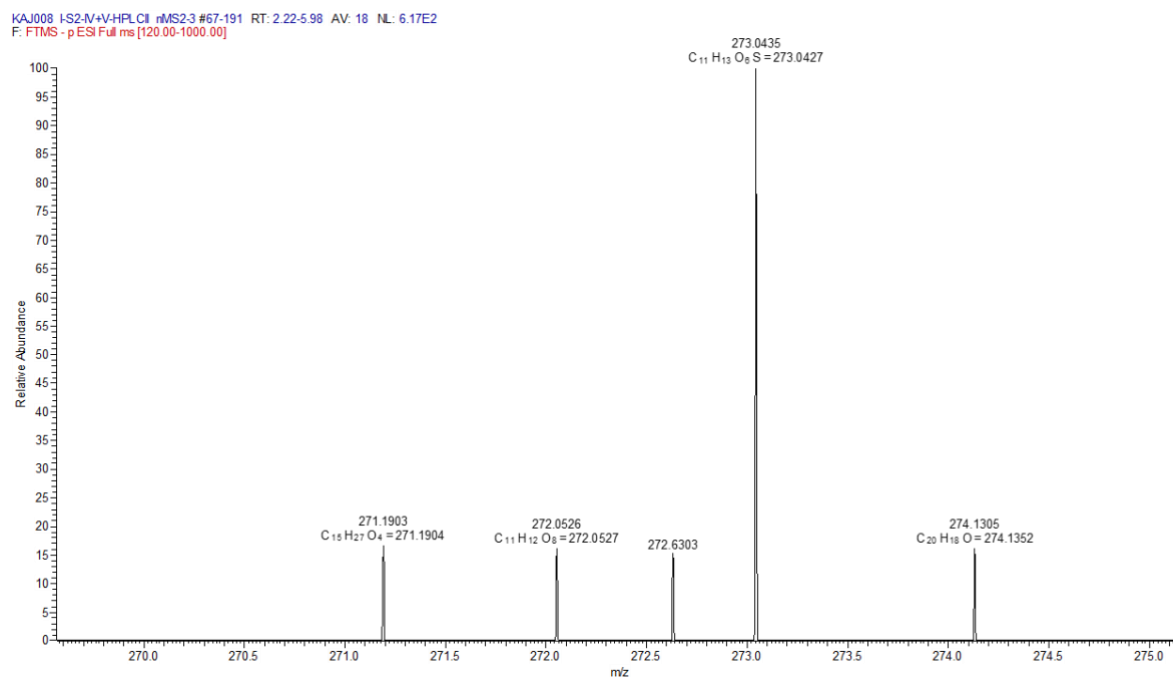


Figure S10-4. HSQC spectrum of 4-(4-sulfoxy-3-methoxyphenyl)-butan-2-one (**4**).**Figure S10-5.** HMBC spectrum of 4-(4-sulfoxy-3-methoxyphenyl)-butan-2-one (**4**).**Figure S10-6.** Full HRMS spectrum of 4-(4-sulfoxy-3-methoxyphenyl)-butan-2-one (**4**) acquired with LIT-Orbitrap-MS in negative ion mode.

KAJ008_I-S2-IV+V-HPLCIL_rMS2-3 #178 RT: 5.76 AV: 1 NL: 1.28E3
F: FTMS - c ESI Full ms2 273.00@cid30.00 [75.00-280.00]

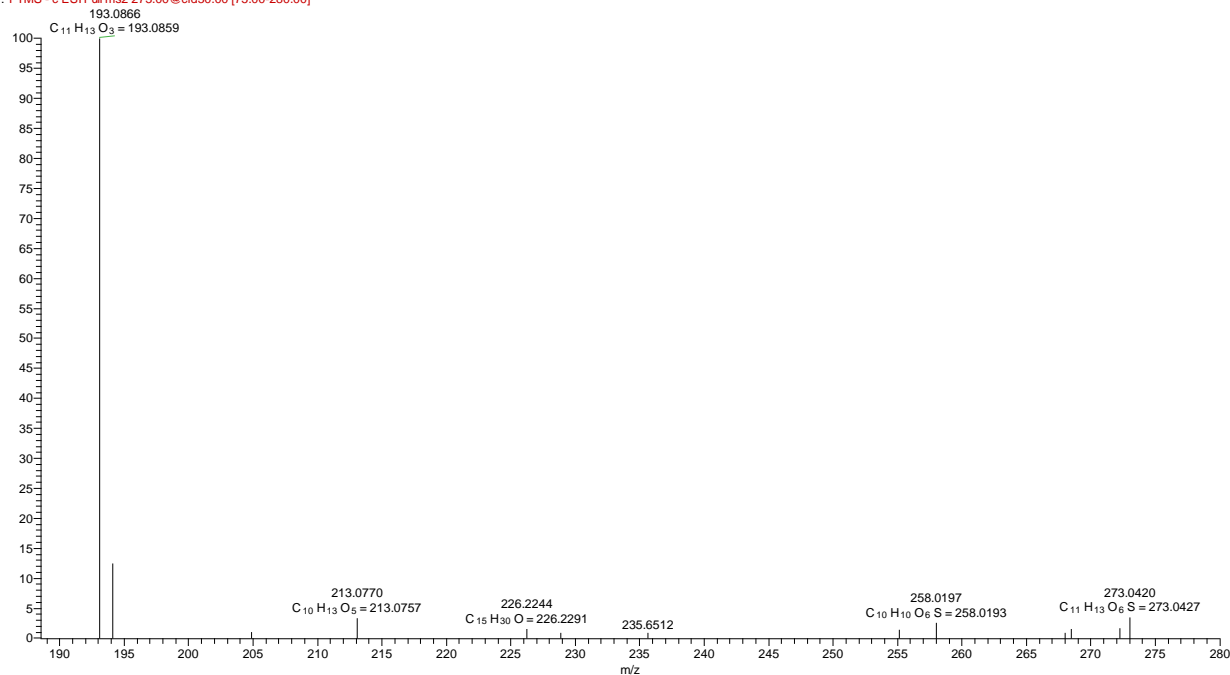


Figure S10-7. MS2 spectrum of 4-(4-sulfoxy-3-methoxyphenyl)-butan-2-one (**4**) acquired with LIT-Orbitrap-MS in negative ion mode with CID activation (35% relative collision energy).

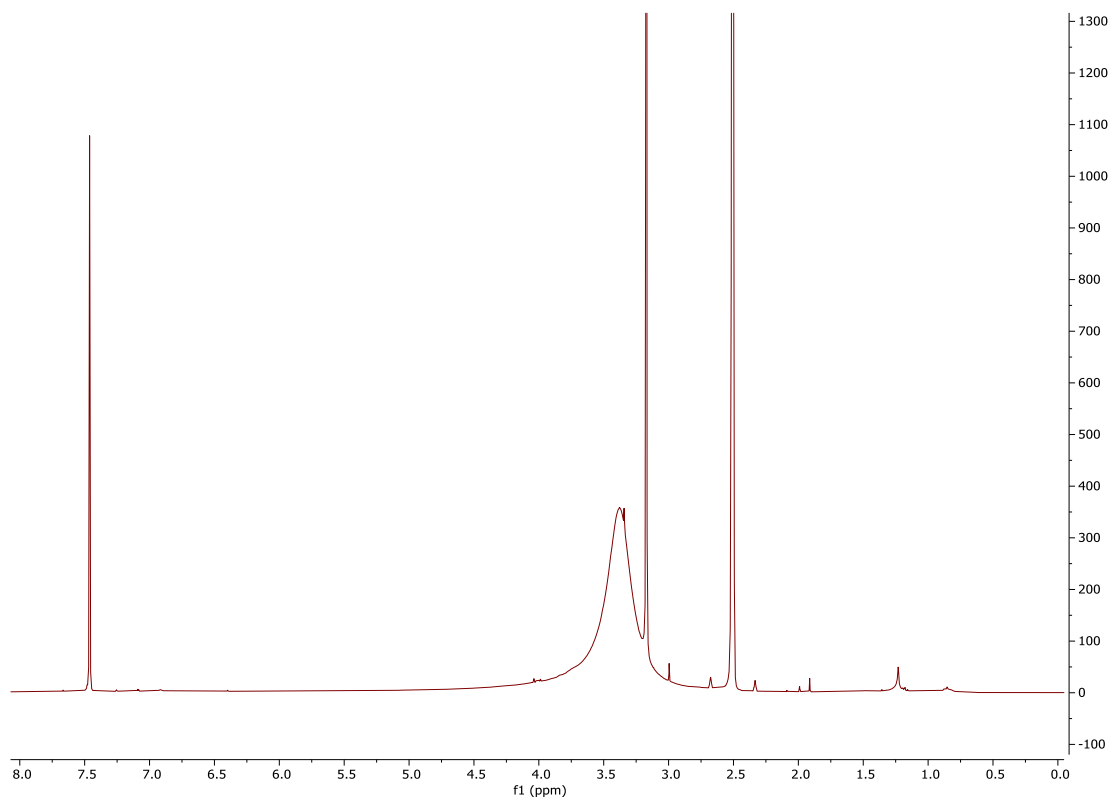


Figure S11-1. ¹H NMR spectrum (DMSO-d₆) of ellagic acid (**7**).

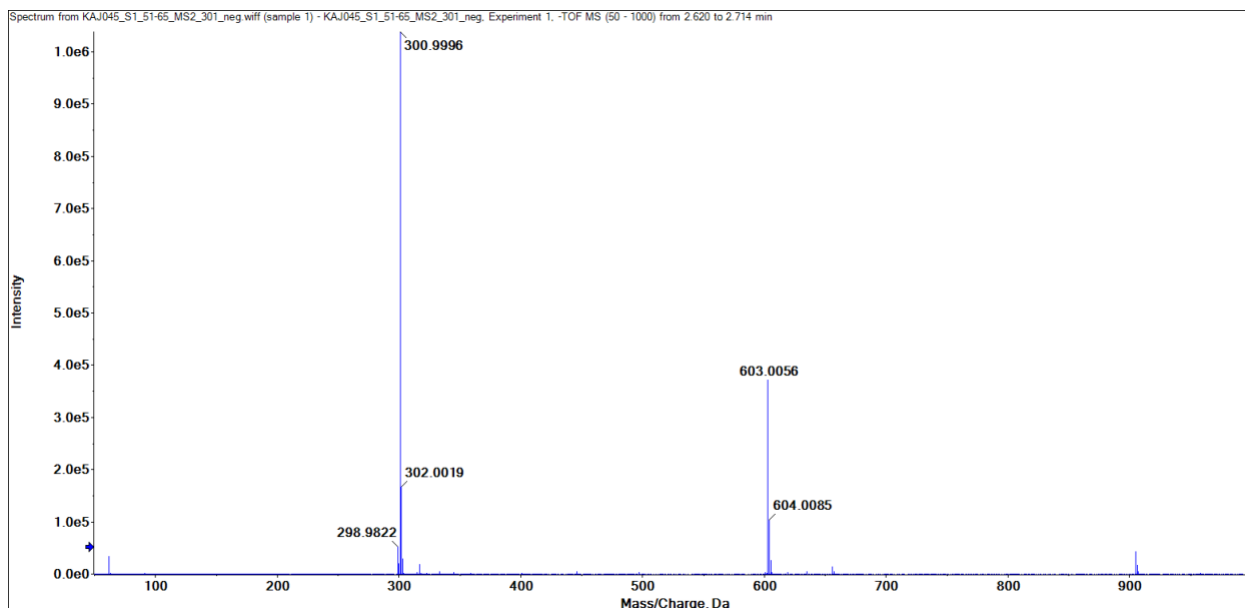


Figure S11-2. HRMS spectrum of ellagic acid (**7**) acquired with a QqTOF mass spectrometer in negative mode.

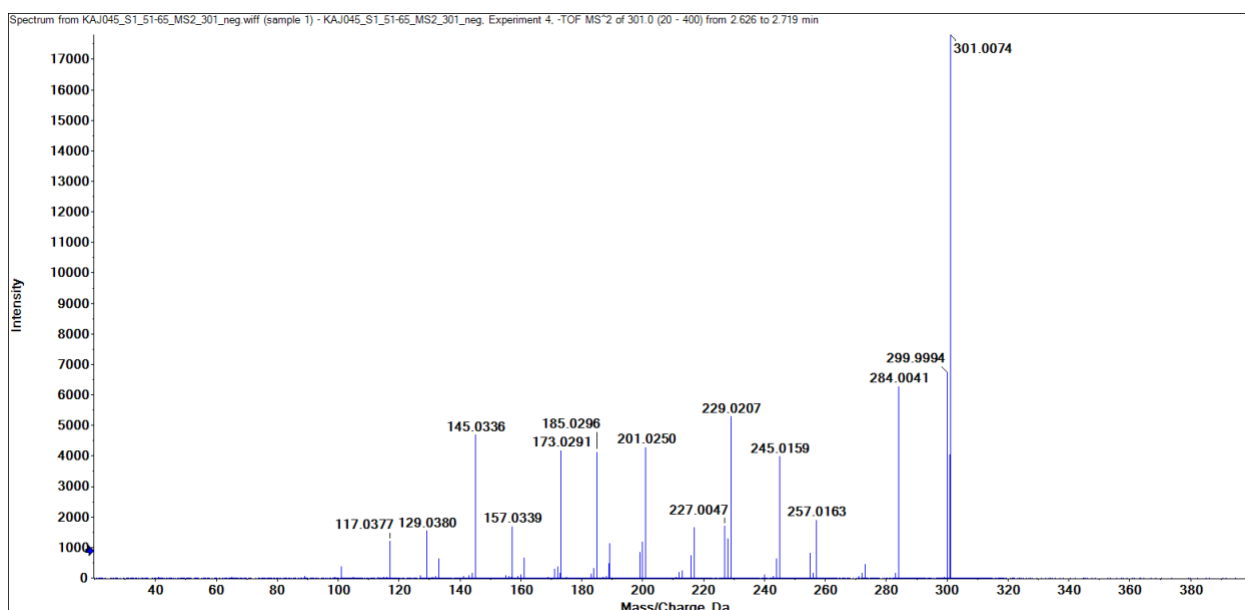


Figure S11-3. MS² spectrum of ellagic acid (**7**) acquired with a QqTOF mass spectrometer in negative mode.

Table S8. NMR spectroscopic data (400 MHz, DMSO-d6) for 3,4-di-*O*-methylellagic acid (**14**).

position	δ_{H} (J in Hz)	δ_{C} *, type	HMBC	ROESY
1		115.00, C		
2		141.79, C		
3		140.04, C		
4		152.73, C		
5	7.53, s	105.83, CH	1, 2, 3, 4, 6, 7	4-O-Me
6		112.95, C		
7		160.22, C		
1'		114.97, C		
2'		134.51, C		
3'		151.92, C		
4'		156.46, C		
5'	7.09, s	104.63, CH	1', 2', 3', 4', 6', 7'	
6'		113.09, C	5'	
7'		159.15, C	5'	
3-OMe	3.99, s	60.83, CH ₃	3	
4-OMe	3.97, s	56.32, CH ₃	4, 5	5

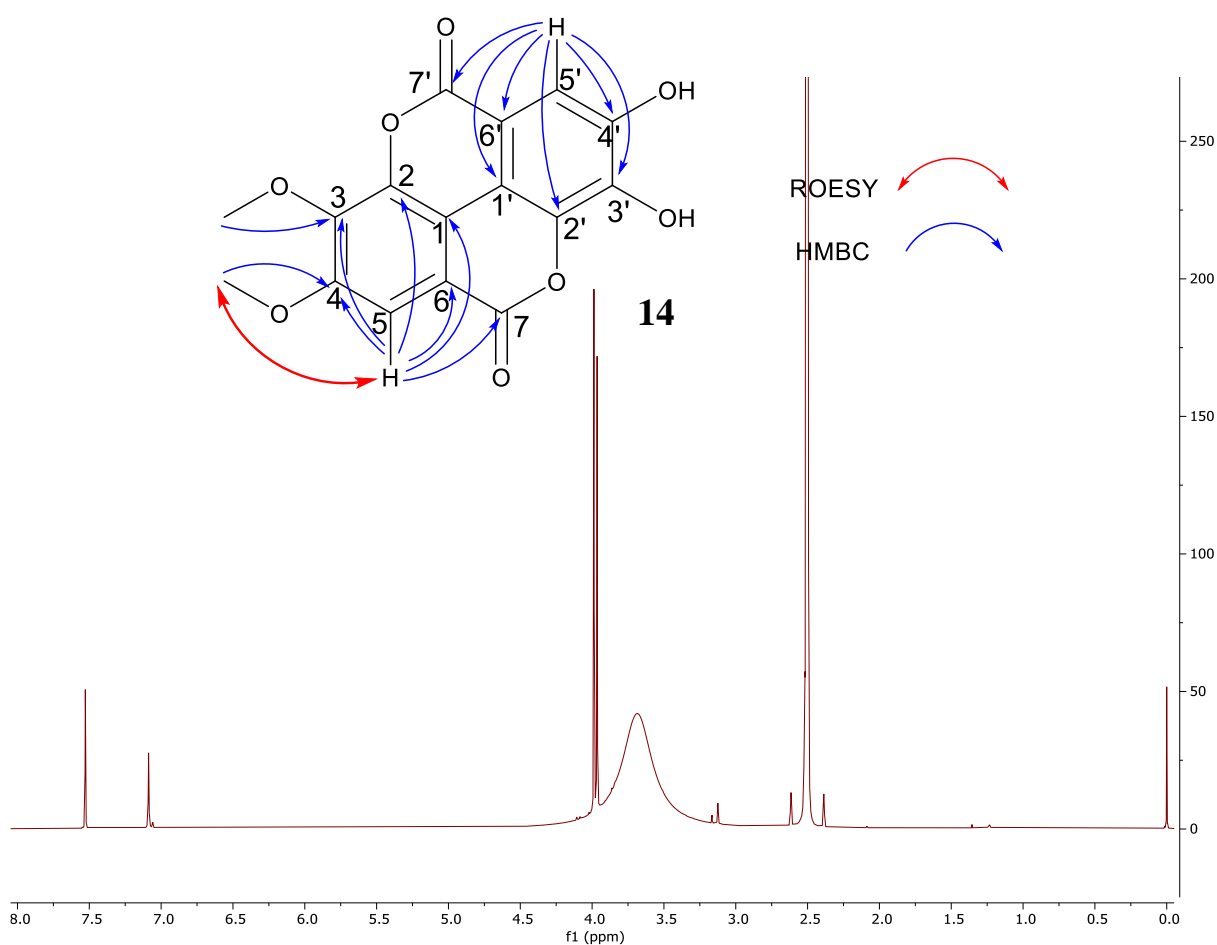


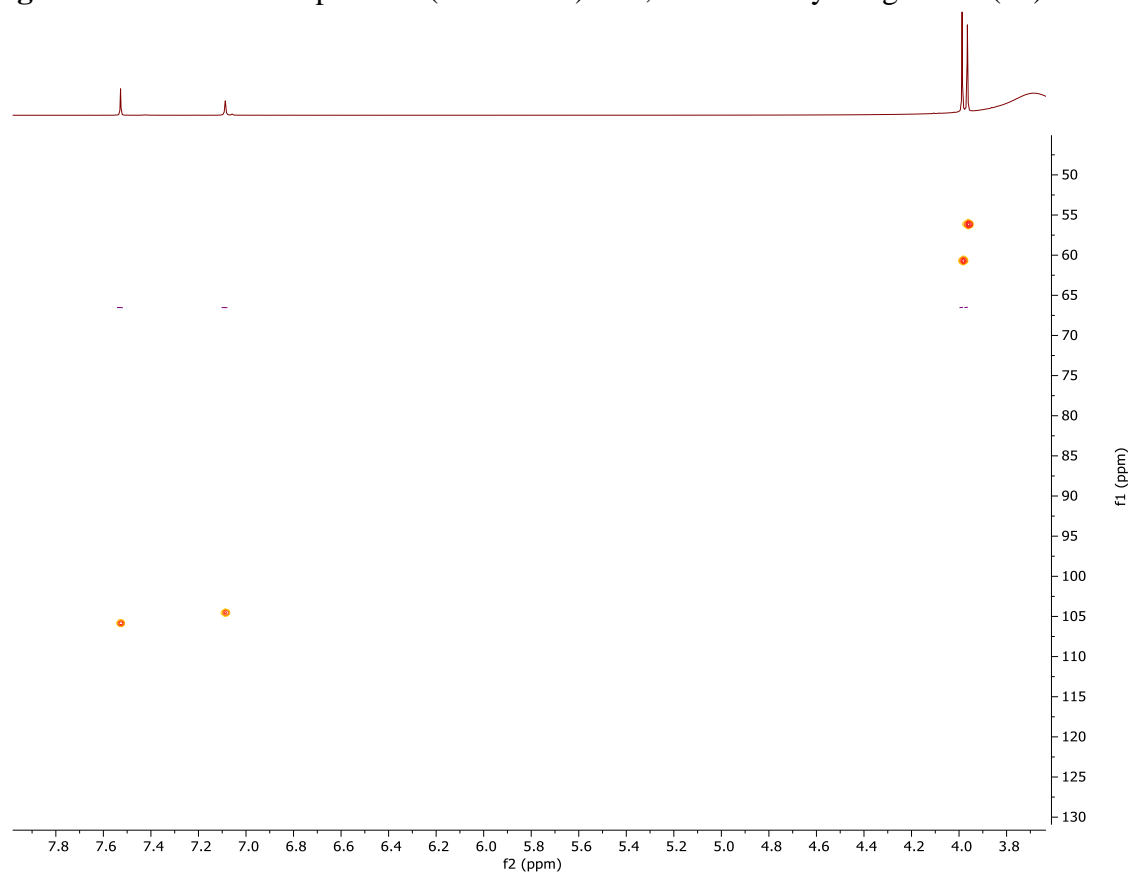
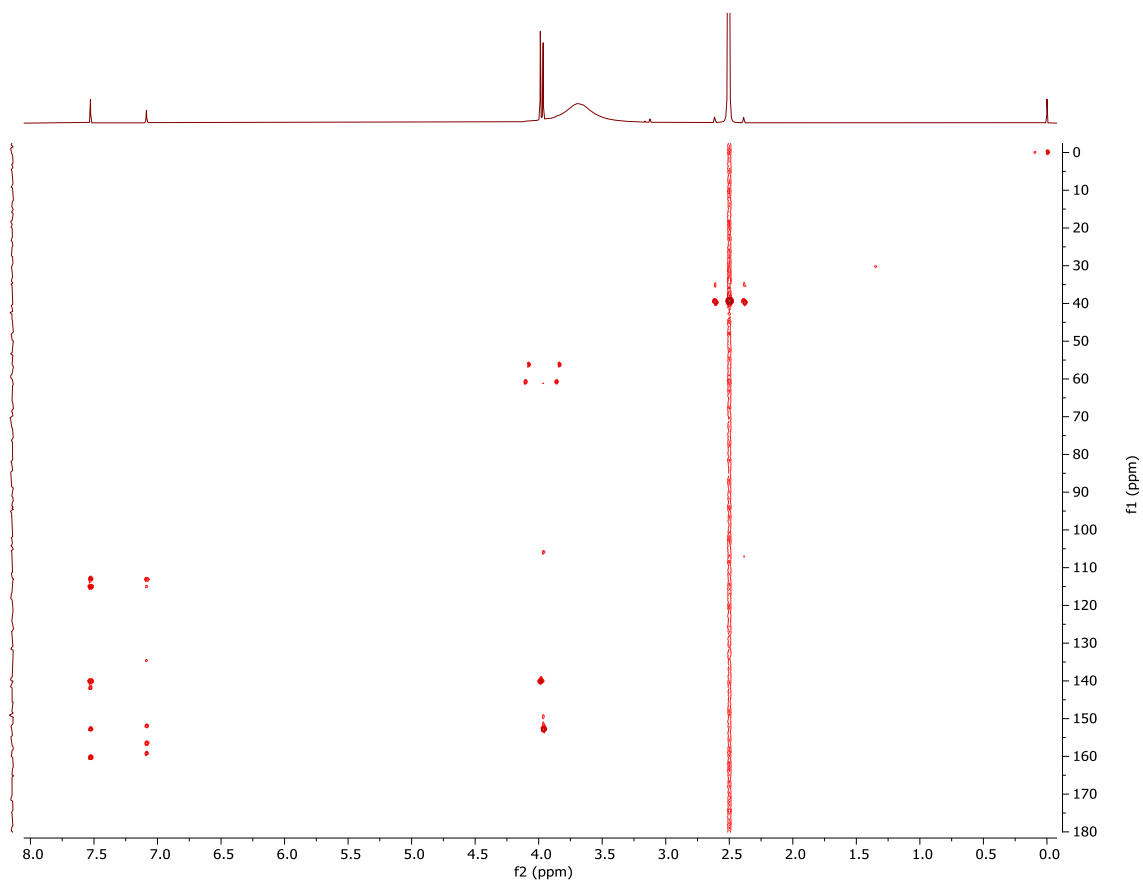
Figure S12-1. ^1H NMR spectrum (DMSO- d_6) of 3,4-di-*O*-methylellagic acid (**14**).**Figure S12-2.** HSQC spectrum (DMSO- d_6) of 3,4-di-*O*-methylellagic acid (**14**).

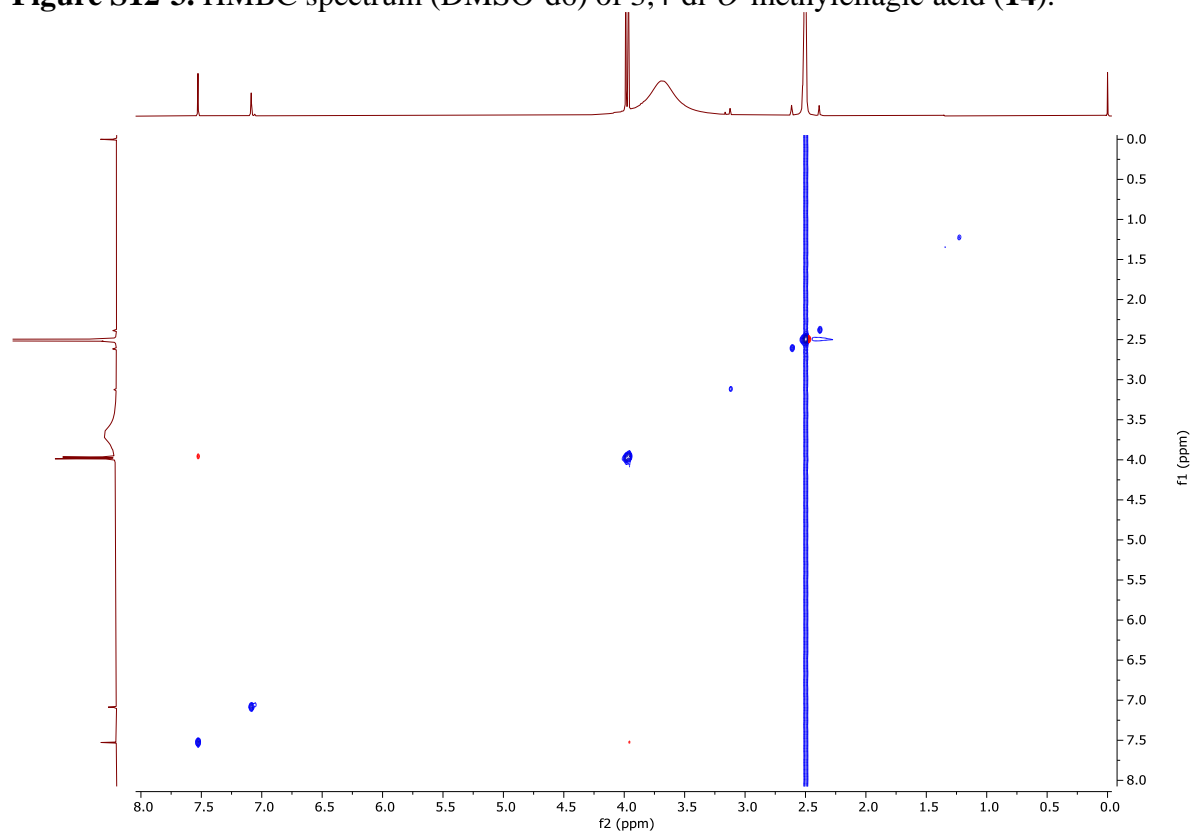
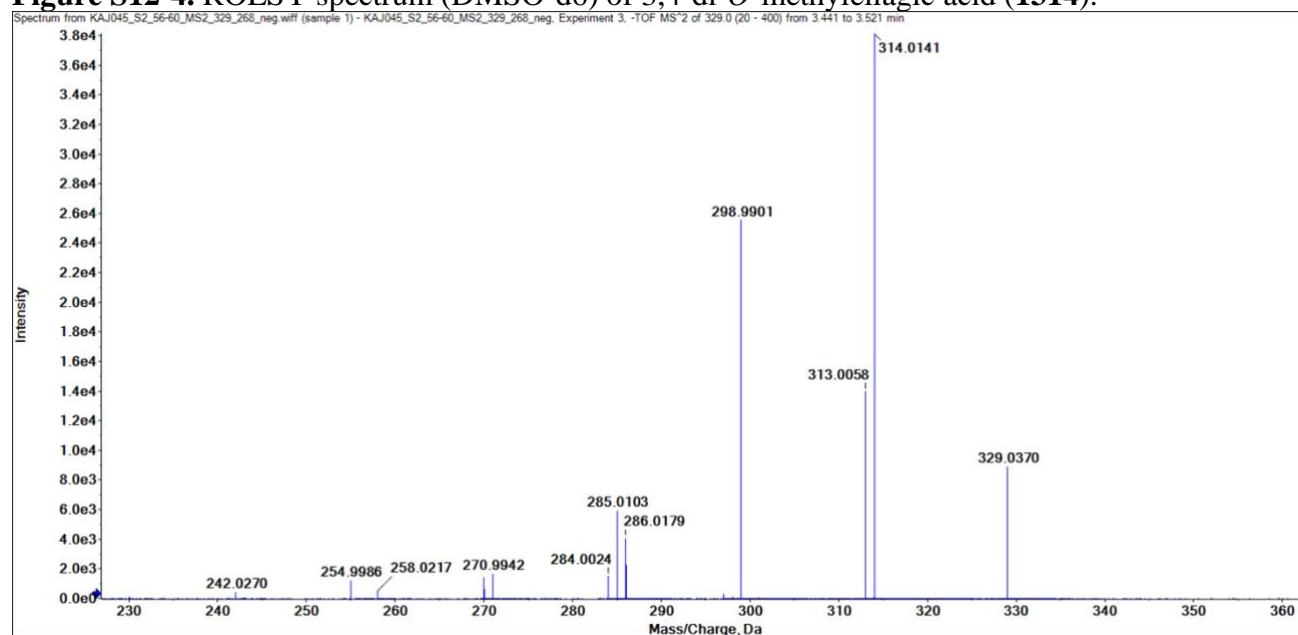
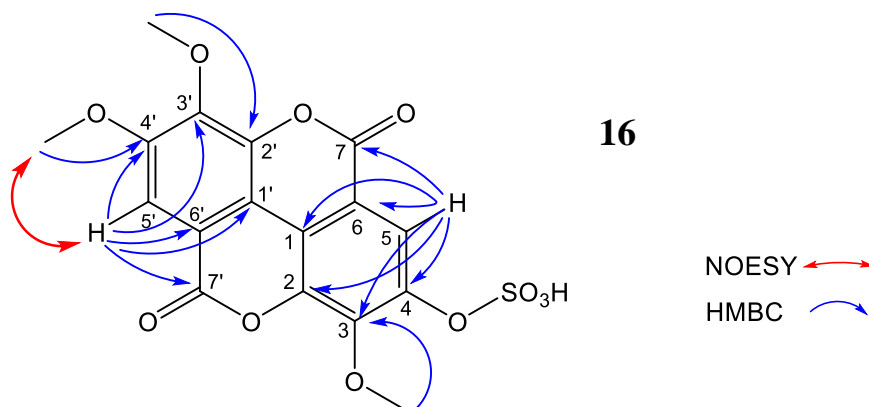
Figure S12-3. HMBC spectrum (DMSO-d₆) of 3,4-di-*O*-methylellagic acid (**14**).**Figure S12-4.** ROESY spectrum (DMSO-d₆) of 3,4-di-*O*-methylellagic acid (**1314**).**Figure S12-5.** MS2 spectrum of 3,4-di-*O*-methylellagic acid (**14**) acquired with a QqTOF mass spectrometer in negative mode.

Table S9. NMR spectroscopic data (400 MHz, DMSO-*d*₆) for 3,3',4'-tri-*O*-methylelagic acid 4-sulfate (**16**).

position	δ_c , type	δ_H	NOESY	HMBC
1	112.96, C			
2	140.86, C			
3	143.32, C			
4	147.64, C			
5	117.61, CH	8.24, s		1, 2, 3, 4, 6, 7
6	111.52, C			
7	158.31, C=O			
1'	114.13, C			
2'	140.89, C			
3'	141.34, C			
4'	154.37, C			
5'	107.50, CH	7.66, s	4'-OMe	1',2', 3', 4', 6', 7'
6'	112.83, C			
7'	158.46, C=O			
3'-OMe	61.32, CH ₃	4.06, s		2'
4'-OMe	56.75, CH ₃	4.02, s	5'	4'
3-OMe	61.47, CH ₃	4.12, s		3



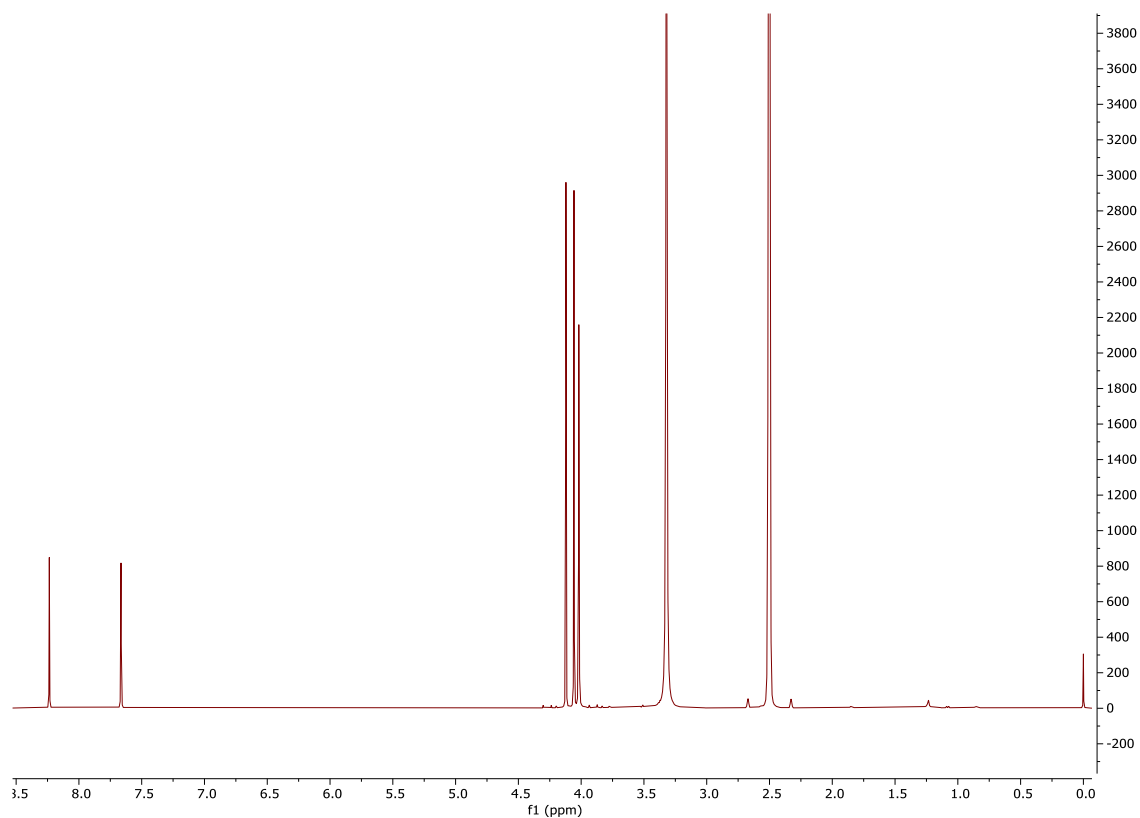


Figure S13-1. ¹H NMR spectrum of 3,3',4'-tri-*O*-methylellagic acid 4-sulfate (**16**).

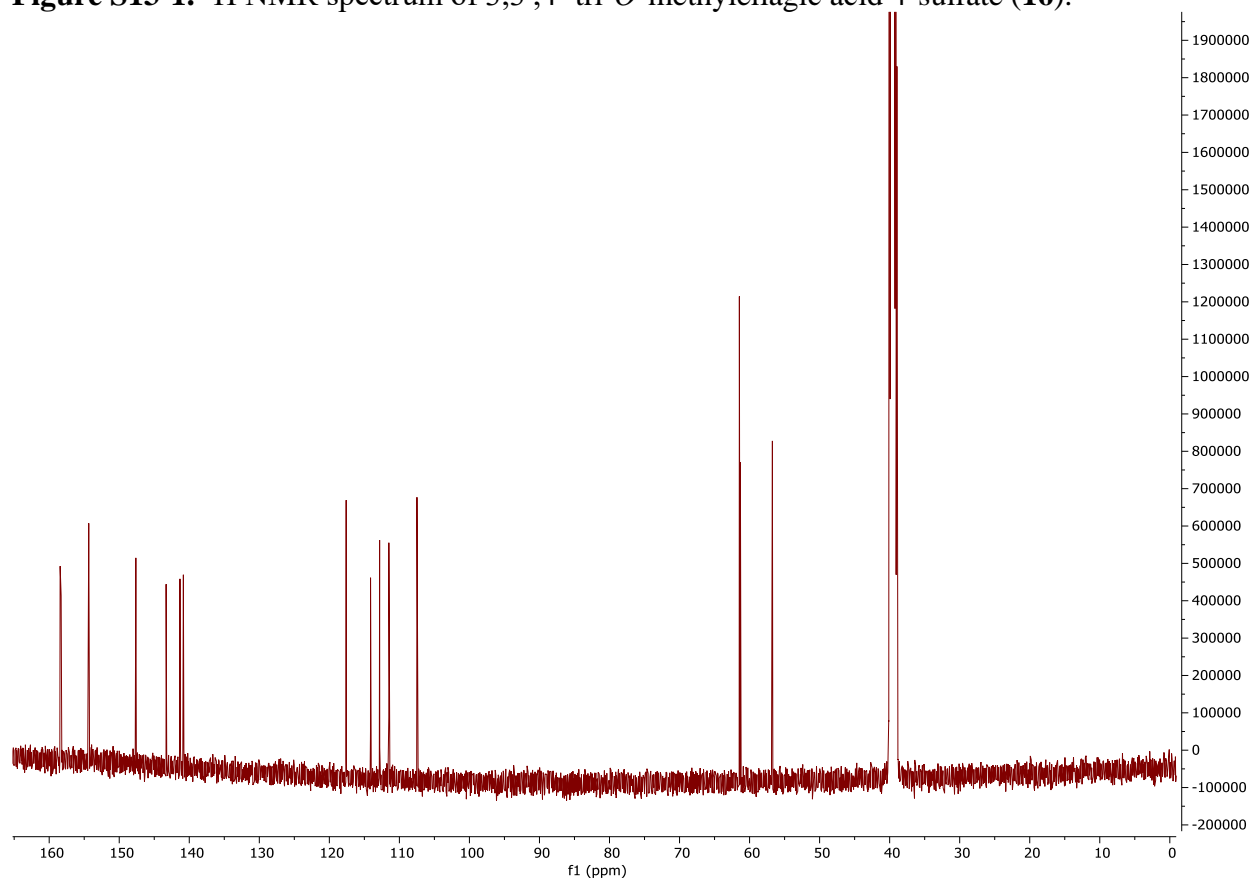


Figure S13-2. ¹³C NMR spectrum of 3,3',4'-tri-*O*-methylellagic acid 4-sulfate (**16**).

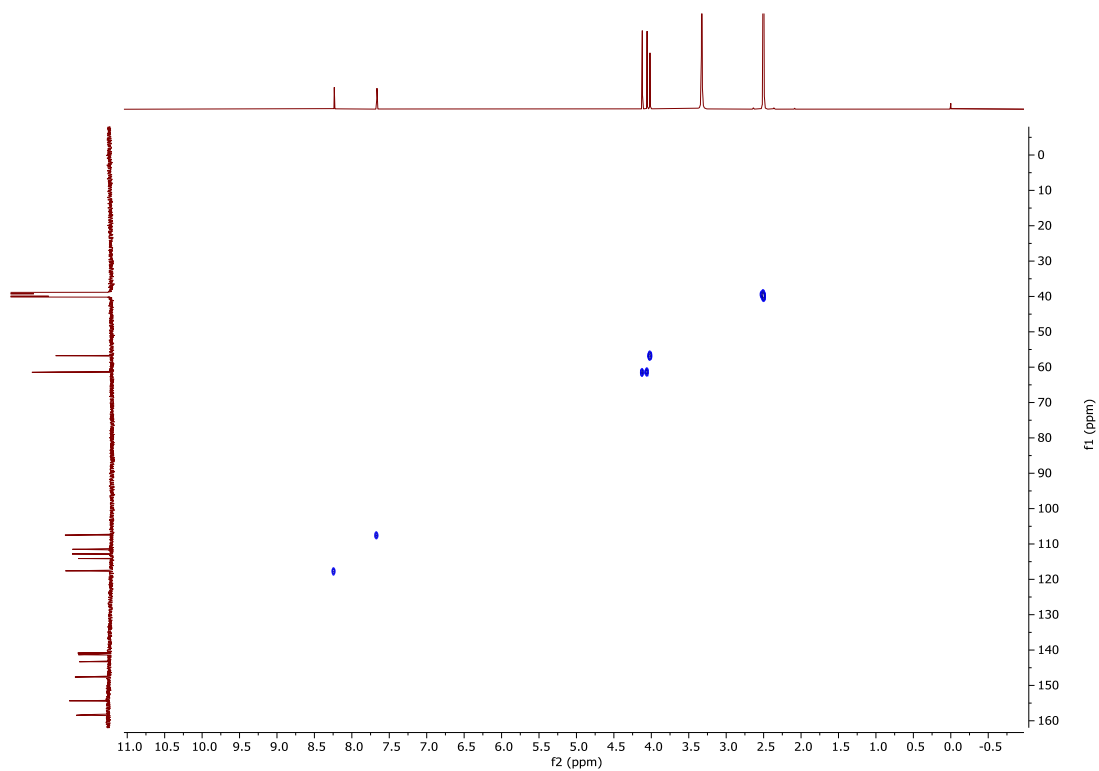


Figure S13-3. HSQC spectrum of 3,3',4'-tri-*O*-methylellagic acid 4-sulfate (**16**).

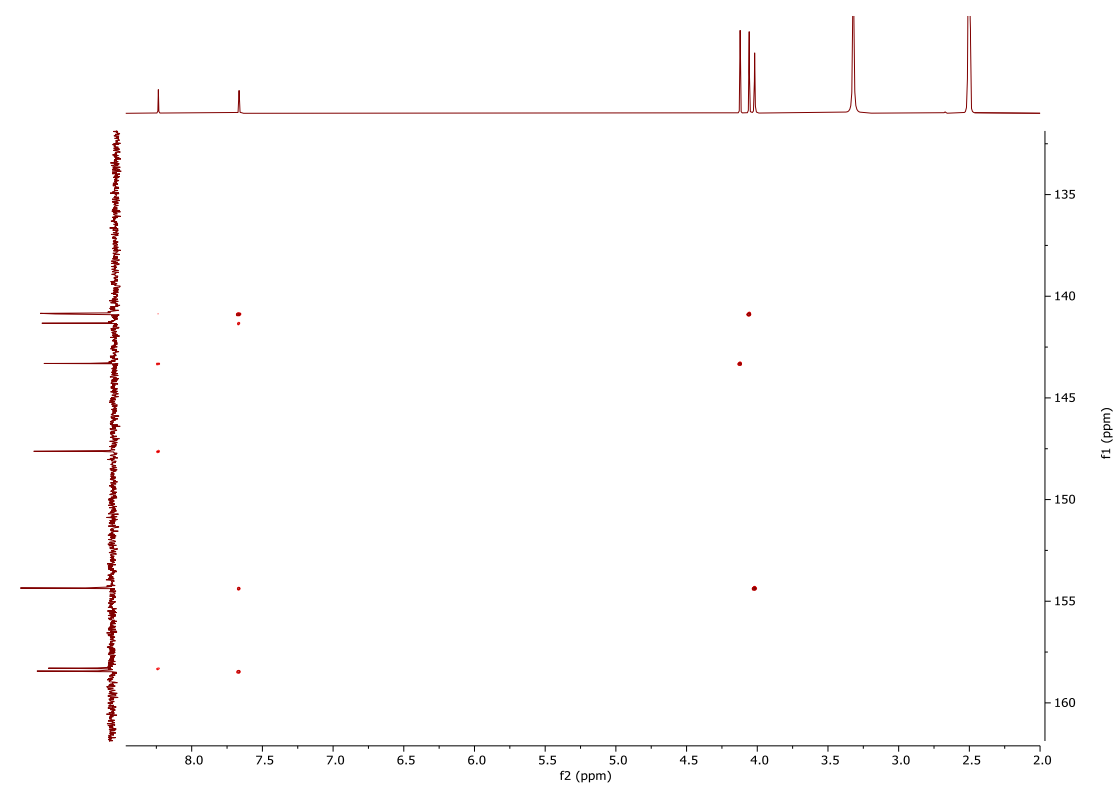


Figure S13-4. HMBC spectrum of 3,3',4'-tri-*O*-methylellagic acid 4-sulfate (**16**).

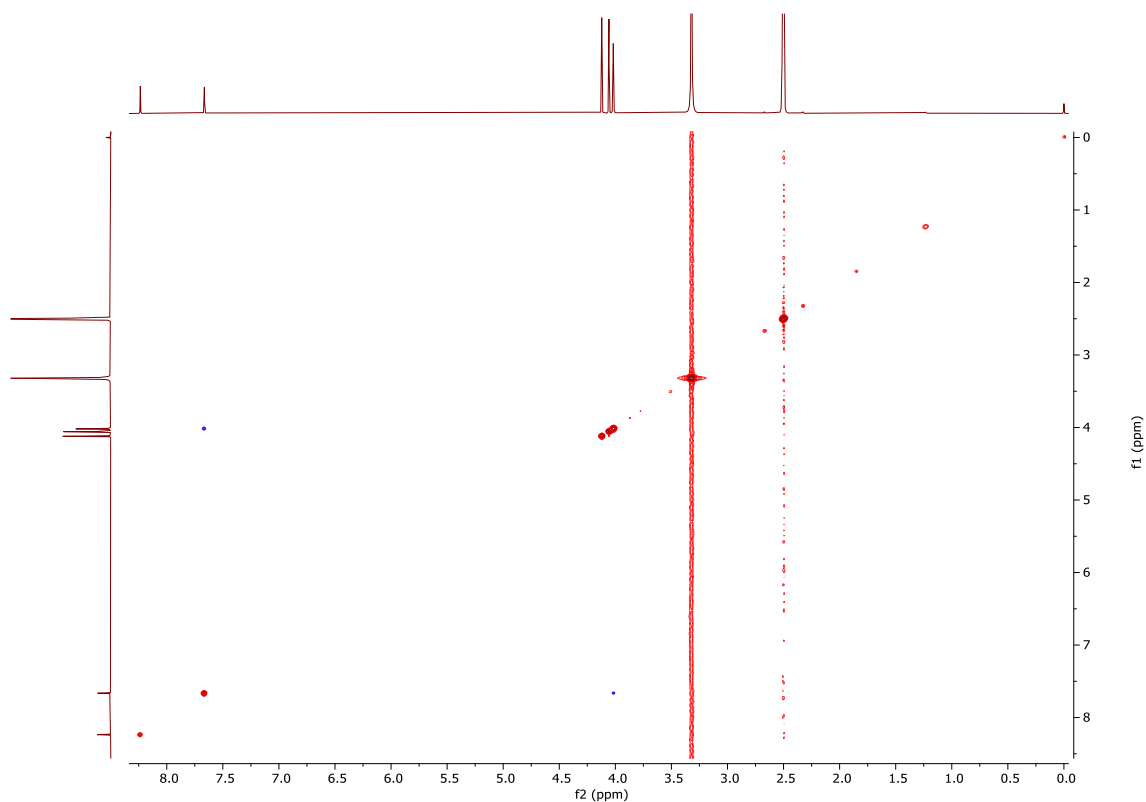


Figure S13-5. NOESY spectrum of 3,3',4'-tri-*O*-methylellagic acid 4-sulfate (**16**).

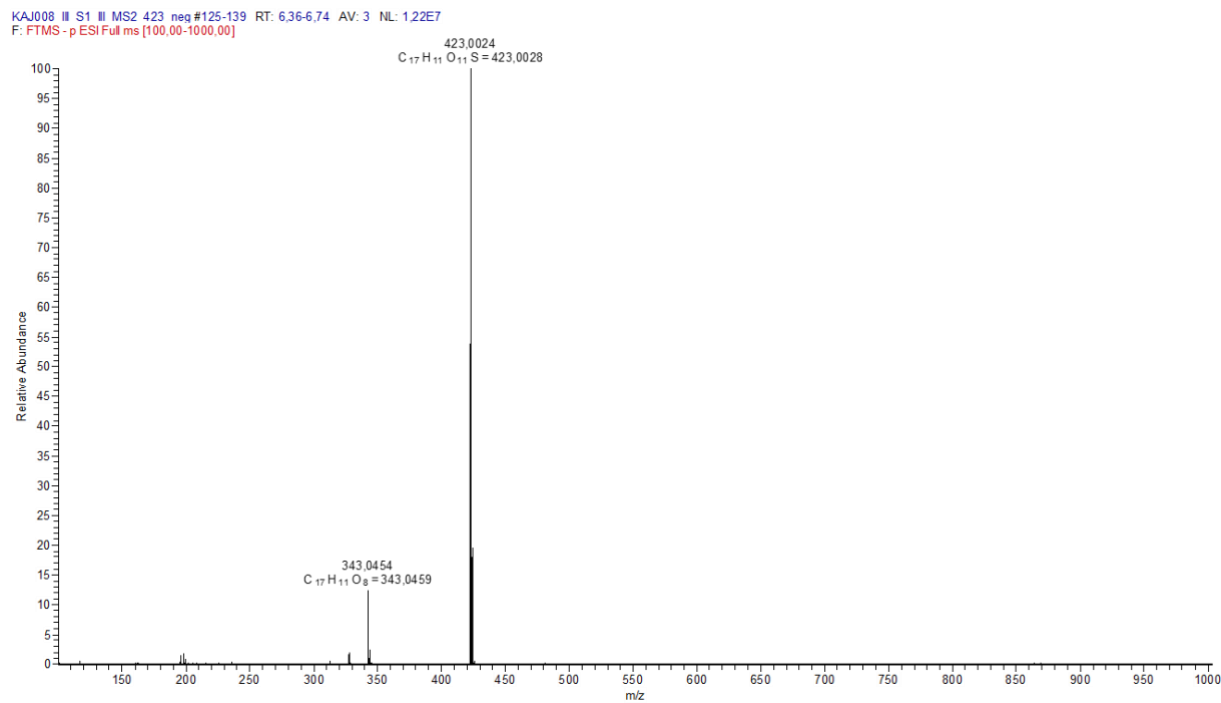


Figure S13-6. Full HRMS spectrum of 3,3',4'-tri-*O*-methylellagic acid 4-sulfate (**16**) acquired with LIT-Orbitrap-MS in negative ion mode.

KAJ008_II_S1_III_MS2_423_neg #128-138 RT: 6.49-6.71 AV: 4 NL: 1.29E7
F: FTMS -p ESI Full ms2 423.00@cid40.00 [300.00-500.00]

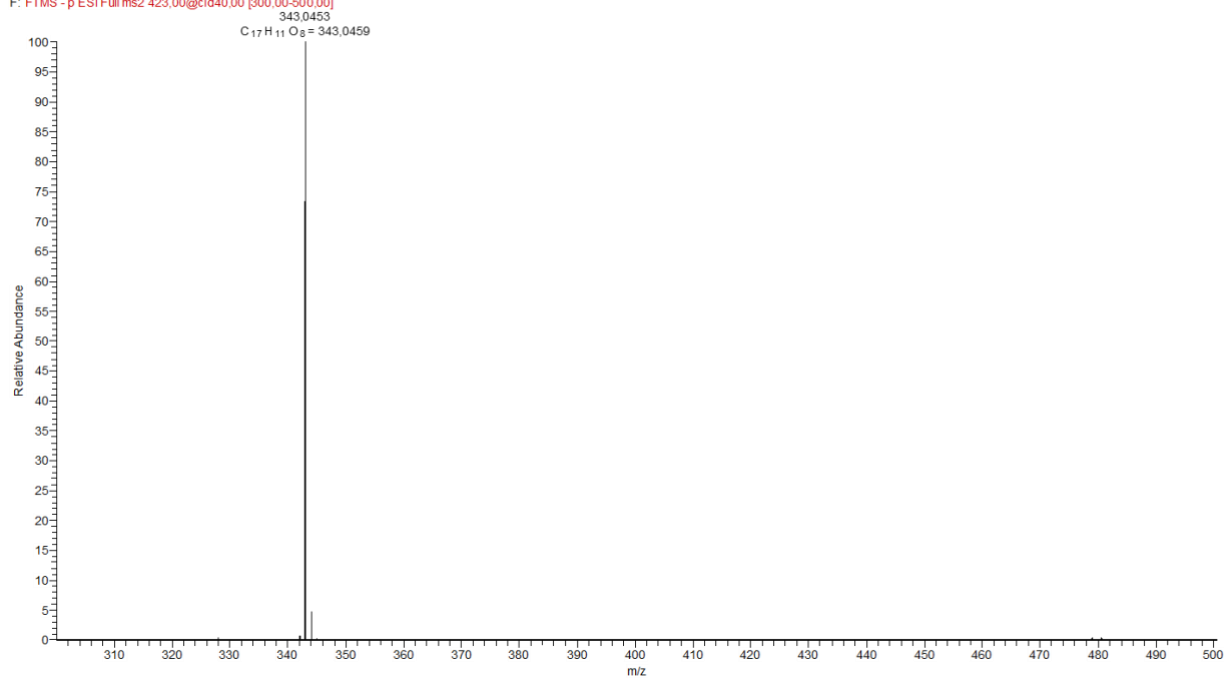
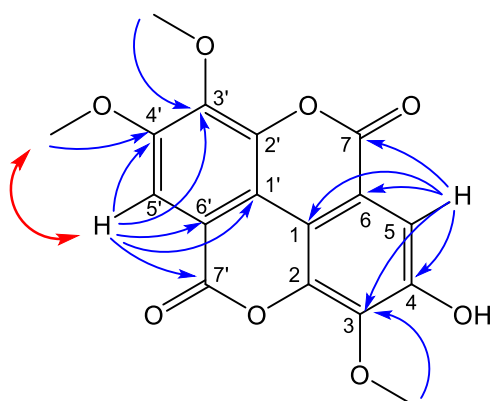



Figure S13-7. MS2 spectrum of 3,3',4'-tri-*O*-methylelagic acid 4-sulfate (**16**) acquired with LIT-Orbitrap-MS in negative ion mode with CID activation (40% relative collision energy).

Table S10. NMR spectroscopic data (400 MHz, DMSO-*d*₆) for 3,3',4'-trimethylellagic acid (**17**).

position	δ_c	δ_H (J in Hz)	NOESY	HMBC
1	110.80, C			
2	140.67, C			
3	140.18, C			
4	152.96, C			
5	111.67, CH	7.52, s		1, 3, 4, 6, 7
6	112.39, C			
7	158.24, C=O			
1'	111.74, C			
2'	141.37, C			
3'	140.85, C			
4'	153.62, C			
5'	107.33, CH	7.61, s	4'-OMe	1', 3', 4', 6', 7'
6'	113.33, C			
7'	158.44, C=O			
3'-OMe	61.19, CH ₃	4.04, s		3'
4'-OMe	56.60, CH ₃	4.00, s	5'	4'
3-OMe	60.83, CH ₃	4.06, s		3

**17**

NOESY 

HMBC 

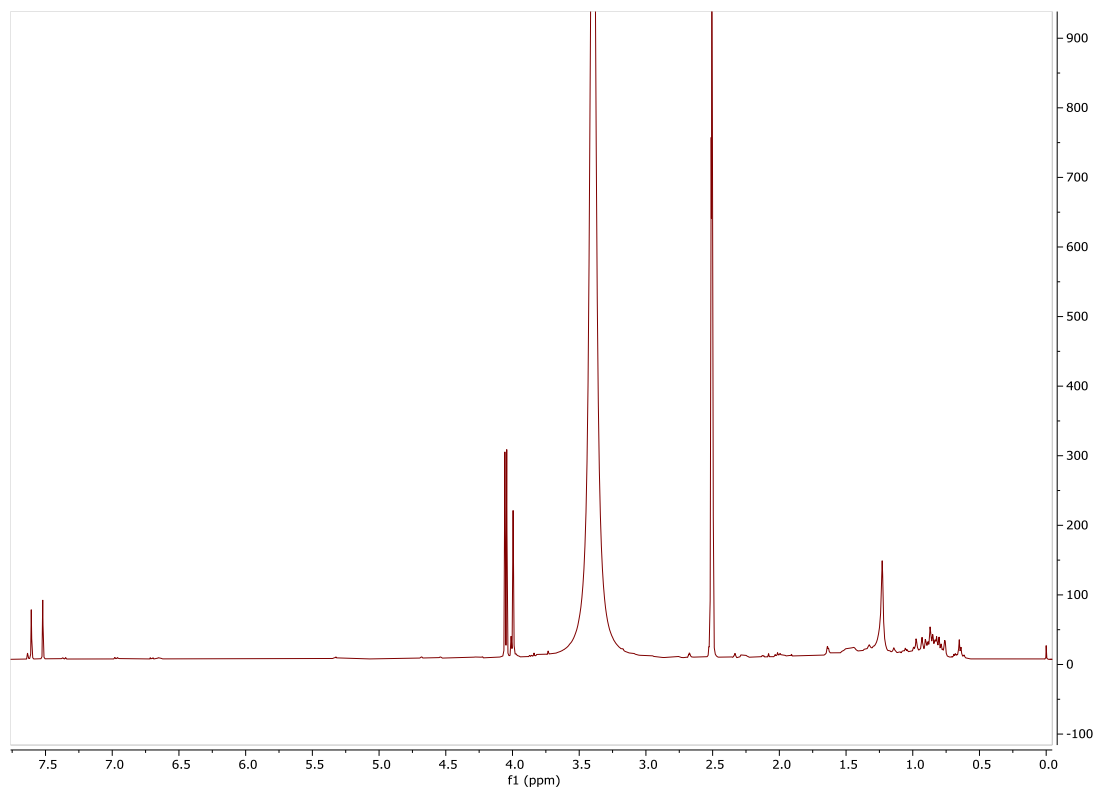


Figure S14-1. ^1H NMR spectrum of 3,3',4'-tri-*O*-methylellagic acid (17).

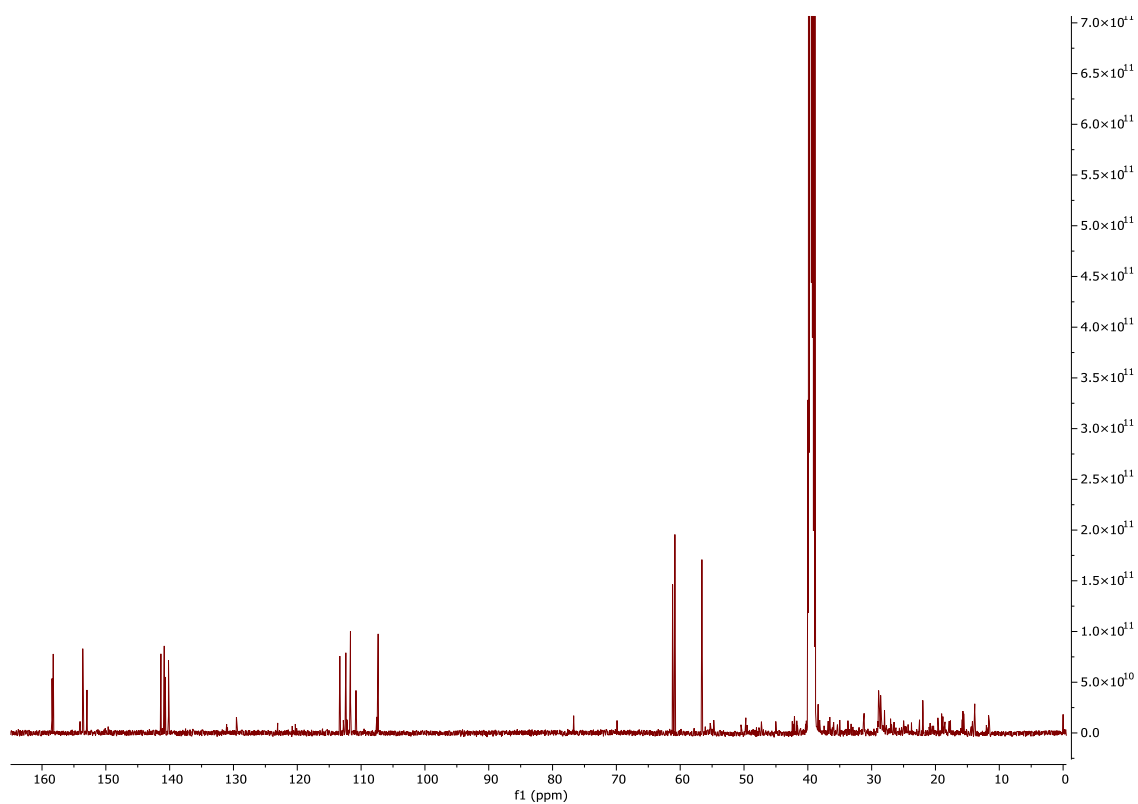


Figure S14-2. ^{13}C NMR spectrum of 3,3',4'-tri-*O*-methylellagic acid (17).

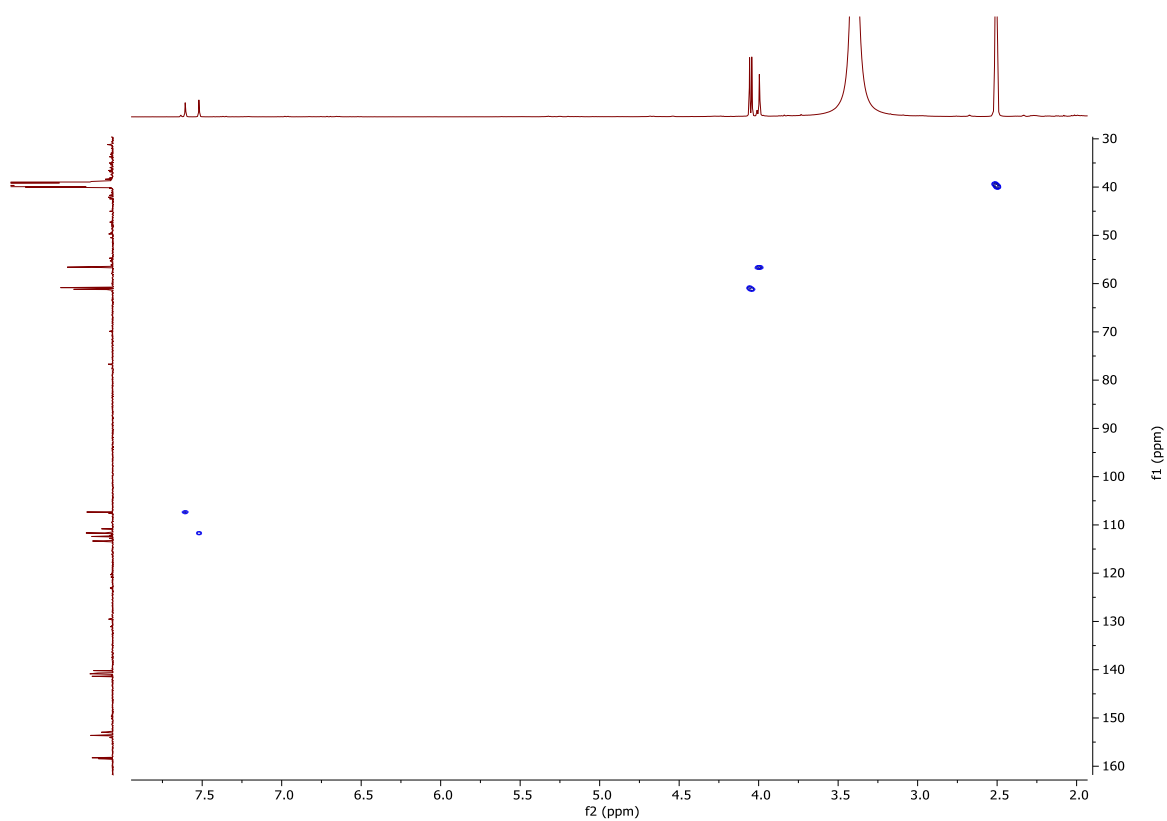


Figure S14-3. HSQC spectrum of 3,3',4'-tri-*O*-methylellagic acid (**17**).

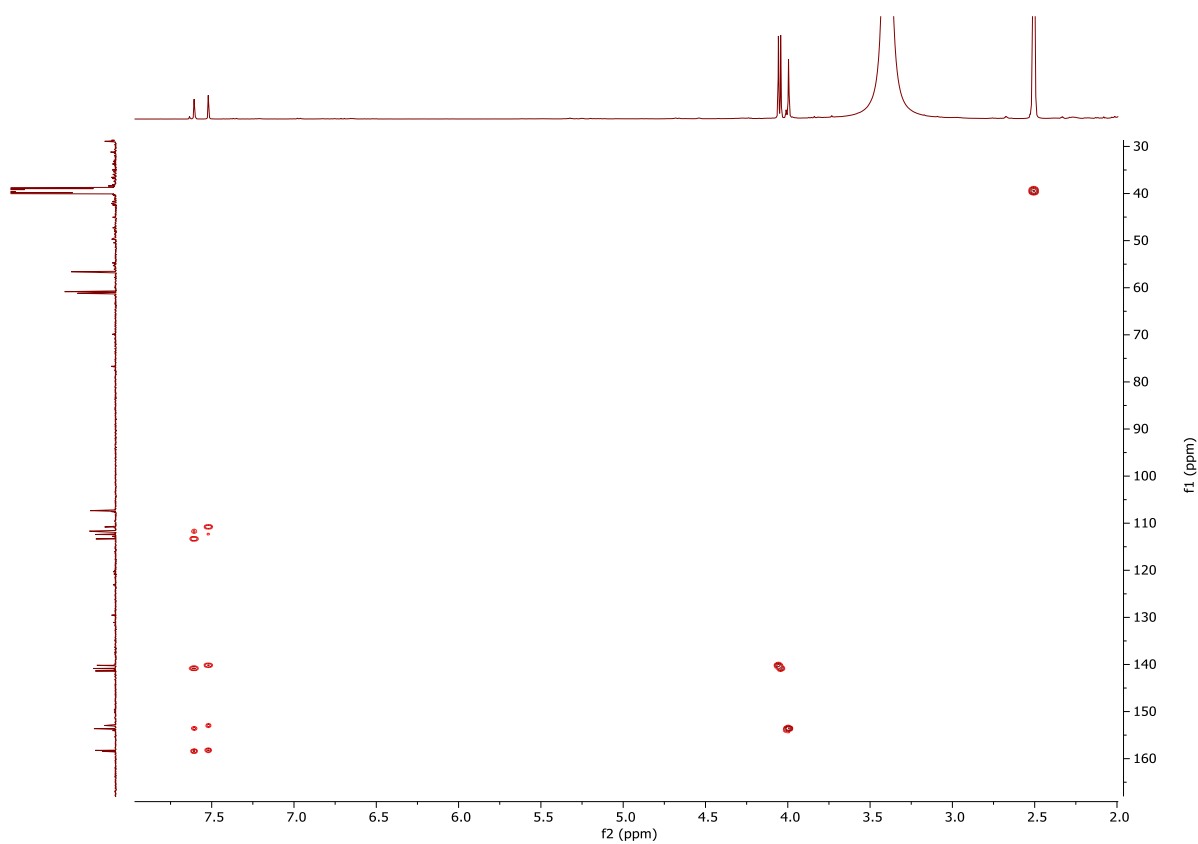


Figure S14-4. HMBC spectrum of 3,3',4'-tri-*O*-methylellagic acid (**17**).

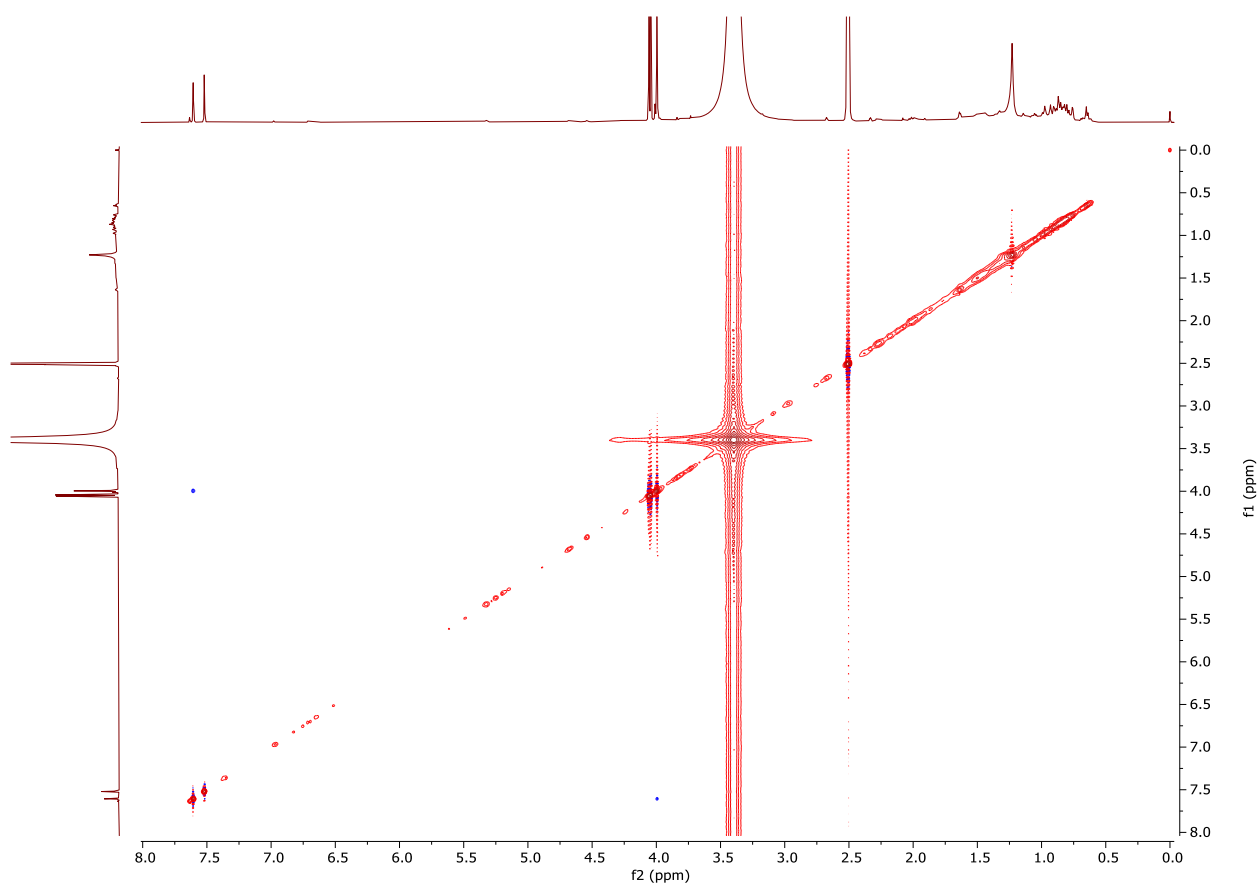


Figure S14-5. NOESY spectrum of 3,3',4'-tri-*O*-methylellagic acid (**17**).

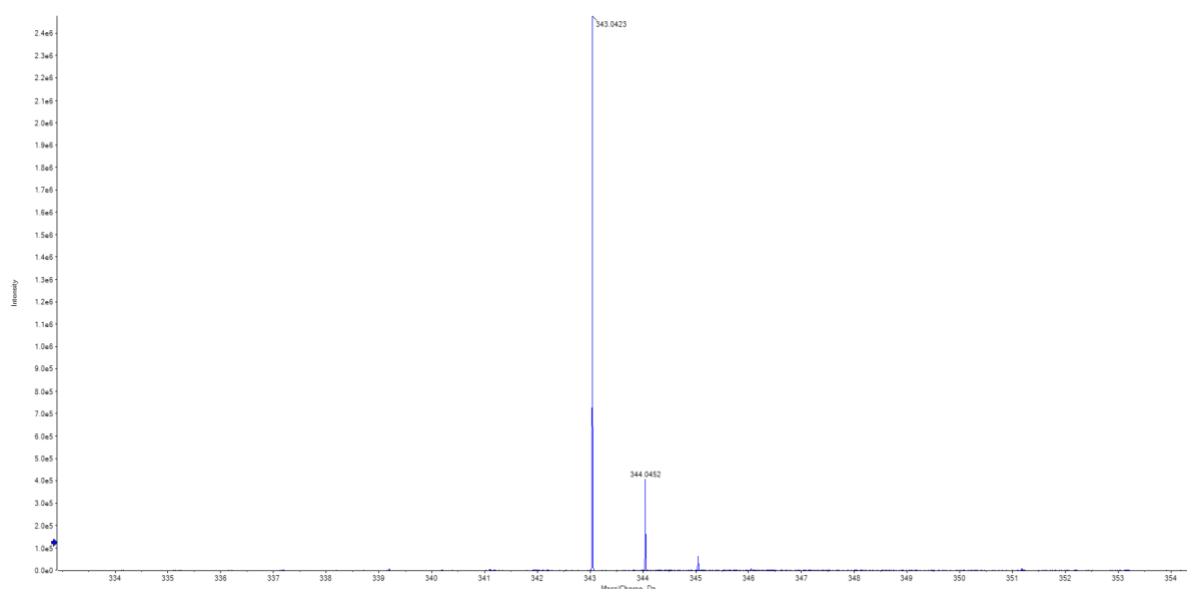


Figure S14-6. Negative HR-MS spectrum of 3,3',4'-tri-*O*-methylellagic acid (**17**) acquired with a QqTOF mass spectrometer.

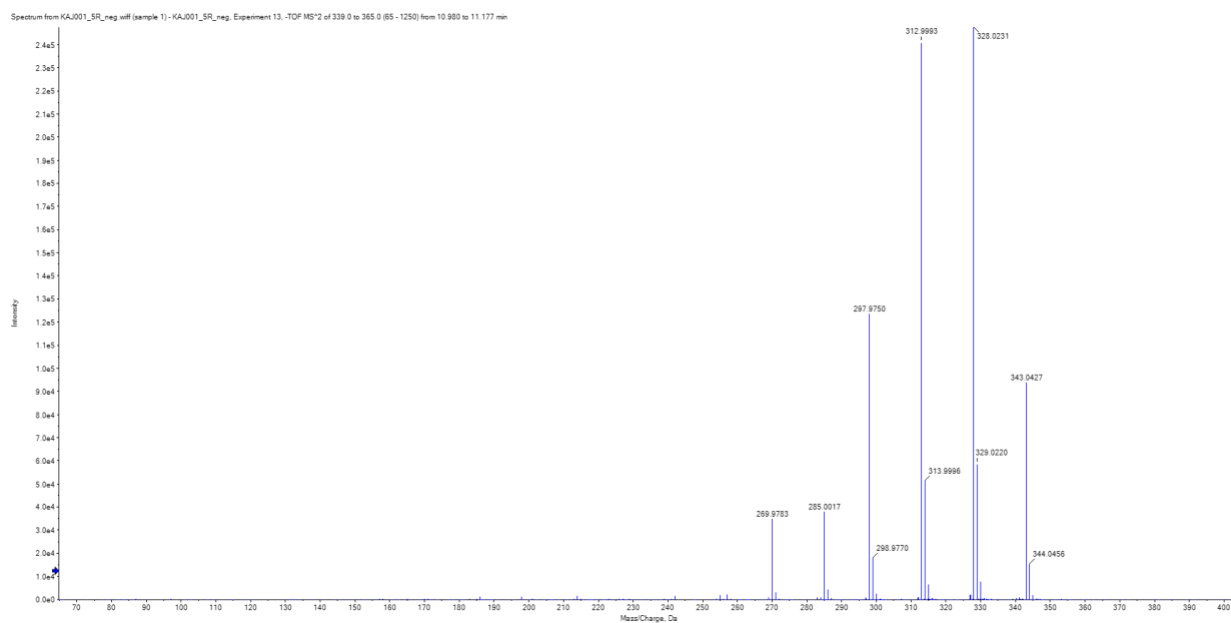


Figure S14-7. MS² spectrum of 3,3',4'-tri-*O*-methylsuccinic acid (**17**), acquired with a QqTOF mass spectrometer in negative mode.